THE JOURNAL OF PHYSICAL CHEMISTRY B
A JOURNAL OF THE AMERICAN CHEMICAL SOCIETY

pubs.acs.org/JPCB

Article

Torsion-Induced Nonradiative Relaxation of the Singlet Excited State of *meso*-Thienyl Bodipy and Charge Separation, Charge Recombination-Induced Intersystem Crossing in Its Compact Electron Donor/Acceptor Dyads

Yu Dong, Maria Taddei, Sandra Doria, Laura Bussotti, Jianzhang Zhao,* Gloria Mazzone,* and Mariangela Di Donato*

Cite This: https://doi.org/10.1021/acs.jpcb.1c00053

Read Online

ACCESS | Metrics & More | Article Recommendations | Supporting Information

ABSTRACT: We prepared a series of *meso*-thienyl boron-dipyrromethene (Bodipy) derivatives to investigate the spin–orbit charge transfer intersystem crossing (SOCT-ISC). The photophysical properties of the compounds were studied by steady-state and femtosecond/nanosecond transient absorption spectroscopy, as well as density functional theory (DFT) computations. Different from the *meso*-phenyl Bodipy analogues, the *meso*-thienyl Bodipy are weakly fluorescent. Based on femtosecond transient absorption and DFT computations, we propose that the torsion of the thienyl group and the distortion of the Bodipy core (19.7 ps) in the S_1 state lead to a conical intersection on the potential energy surface as an efficient nonradiative decay channel (408 ps), which is responsible for the observed weak fluorescence as compared to the *meso*-phenyl analogue. The increased fluorescence quantum yield (from 5.5 to 14.5%) in viscous solvents supports this hypothesis. With the electron donor 4′-hydroxylphenyl moiety attached to the *meso*-thienyl unit, the fast charge separation (CS, 15.3 ps) and charge recombination (CR, 238 ps) processes outcompete the torsion-induced nonradiative decay and induce fast ISC through the SOCT-ISC mechanism. The triplet quantum yield of the electron donor/acceptor dyad is highly dependent on solvent polarity (Φ_T = 1.9–45%), which supports the SOCT-ISC mechanism, and the triplet-state lifetime is up to 247.3 μs. Using the electron donor–acceptor dyad showing SOCT-ISC as a triplet photosensitizer, efficient triplet–triplet annihilation (TTA) upconversion was observed with a quantum yield of up to 6.0%.

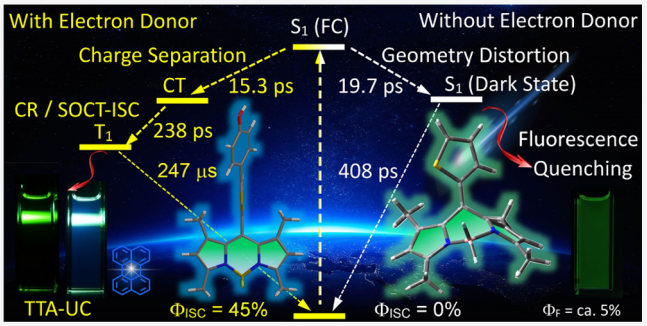

1. INTRODUCTION

Triplet photosensitizers (PSs) are important in fundamental photochemistry studies as well as in photodynamic therapy (PDT),[1−6] photocatalysis,[7−11] photovoltaics,[12−15] and photon upconversion.[16−18] PSs showing strong visible light absorption, efficient intersystem crossing (ISC), and long triplet-state lifetime are highly desired. However, ISC is nonefficient for most aromatic chromophores with large planar π-conjugation systems. The most commonly used method to enhance the ISC is based on the heavy atom effect, obtained by introducing precious metal atoms, such as Pt, Pd, Ir, and Au.[10,19−21] However, problems arise because of the high cost and toxicity of these metals. Halogen atoms, such as I and Br, are also used for similar purposes.[22−24] One of the major drawbacks of this approach is that although the triplet quantum yield is increased, the triplet-state lifetime is shortened since both the $S_1 \rightarrow T_1$ and the $T_1 \rightarrow S_0$ transitions are enhanced by the heavy atom effect. A short triplet-state lifetime is detrimental to the application of the triplet PSs, and in addition, the toxicity of heavy atoms (I, Br) limits their use in biological applications, for instance, in PDT. To overcome these limitations, new methods to achieve efficient ISC using heavy atom-free molecular structures are highly desired, but the related reports are still not abundant.

Charge recombination (CR)-induced ISC has been known for decades,[25−28] but the synthesis of conventional donor–acceptor dyads is complicated because of the large distance necessary to make the radical pair ISC (RP-ISC) possible. Furthermore, in most cases, the ISC and the triplet-state properties of these systems are not studied in detail.[29] Recently, CR-induced ISC in compact, orthogonal electron

Received: January 4, 2021
Revised: April 9, 2021

Scheme 1. Molecular Structures of the Main Compounds Used in the Study

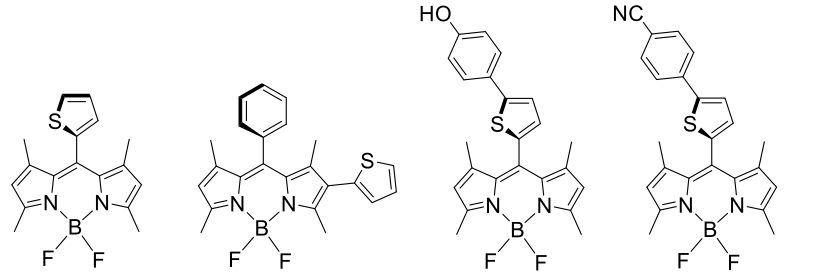

donor/acceptor dyads has attracted much attention. This mechanism, termed as spin−orbit charge transfer ISC (SOCT-ISC),[30−33] does not require heavy atoms in the molecular structures.[34] Several reports are available with the application of this mechanism. For instance, Williegen reported that acridinium−naphthaline dyads showed weak fluorescence and enhanced ISC ability.[31] Wasielewski et al. reported dyads based on anthracene and julolidine moieties, and the geometry factors controlling the ISC efficiency were discussed.[32,35] The studies on Bodipy−anthracene dyads demonstrated the potential application of these compact dyads in PDT.[36] Recently, several SOCT-ISC-based triplet PSs have been reported, obtained by connecting strong electron donors, such as phenothiazine or perylene, to visible light-harvesting chromophores, such as Bodipy and perylenemonoimide.[37−40] The excellent visible light-harvesting ability of these PSs provides the possibility of their use in a practical sense. Until now, the most used electron donors or acceptors have been limited to phenothiazine, phenoxazine, or anthracene. To the best of our knowledge, the thiophene moiety, widely used in organic electro-optic materials, has not been considered in applications concerning the SOCT-ISC.

The excited-state dynamics of Bodipy chromophores has been widely investigated. Although these chromophores are generally highly fluorescent, it has been found that some *meso*-aryl-substituted Bodipy compounds lacking 1,7-dimethyl groups have very low fluorescence quantum yields.[41−44] An empirical explanation for this finding is that the rotation of the *meso*-phenyl substituent dissipates the excited state energy, leading to the quenching of the fluorescence. However, theoretical computations and ultrafast transient absorption spectral studies indicated that the distortion of the Bodipy core at the excited state creates a conical intersection among the S_1 and S_0 states,[45,46] which is responsible for the fast nonradiative decay of the S_1 state. Some *meso*-thienyl Bodipy derivatives have been recently synthesized, and their fluorescence quantum yield has been found quite low. However, transient absorption measurements and theoretical computations aimed at analyzing their nonradiative decay mechanisms have not been reported.[47−50]

To address the above challenges, herein, we prepared four thienyl−Bodipy dyads and studied in detail the photophysical properties (Scheme 1). Bodipy is known for its strong absorption of visible light and high fluorescence quantum yields.[51,52] The thienyl moiety was attached either at the *meso*-position or at the 2-position, and for two compounds, a 4′-hydroxylphenyl or 4′-cyanophenyl group was further linked to the thienyl unit to tune the electron-donating/accepting ability of the substituent. The photophysical properties of these systems were studied with steady-state and time-resolved transient spectroscopy and DFT computations. We found that, different from what is observed in the case of *meso*-phenyl Bodipys, the nonradiative decay is highly efficient for the *meso*-thienyl Bodipy compounds, also in the case of 1,7-dimethyl substitution on the Bodipy core. When an electron-donating 4′-hydroxylphenyl moiety is attached to the thienyl substituent, we observed fast charge separation (CS) and CR, followed by CR-induced ISC, which, for one dyad, produced a long-lived triplet state.

2. EXPERIMENTAL SECTION

2.1. Materials and Equipment. All chemicals are analytically pure. Solvents for synthesis were freshly dried over suitable drying agents before use. ^{1}H and ^{13}C NMR spectra were recorded on Bruker spectrometer at 400 and 100 MHz, respectively. High-resolution mass spectrometry (HRMS) was performed by an EI-TOF-HRMS spectrometer. UV−vis spectra were recorded on an Agilent 8453A UV−vis spectrophotometer (Agilent Ltd.). Fluorescence spectra were recorded on an FS5 spectrophotometer (Edinburgh Instrument Ltd., U.K.). Fluorescence lifetimes were recorded on an OB920 luminescence lifetime spectrometer (Edinburgh Instruments Ltd., U.K.); the excitation sources are the 445 nm (max. pulse width is 95 ps) and 510 nm (max. pulse width is 150 ps) EPL picosecond pulsed diode lasers. A deconvolution analysis was used for fitting the short fluorescence lifetimes with the instrumental response function (IRF) included. The typical IRF of the luminescence lifetime measurement is 100 ps.

2.2. Synthesis of Compound 1.[53] *p*-Bromobenzonitrile (182.0 mg, 1.0 mmol), 5-formyl-2-thiopheneboronic acid (234.0 mg, 1.5 mmol), and Na_2CO_3 (212 mg, 2.0 mmol) were dissolved in dimethyl ether (15 mL) and water (1 mL). After adding $Pd(PPh_3)_4$ (57.7 mg, 0.05 mmol) under a N_2 atmosphere, the reaction mixture was refluxed for 8 h. The crude product was dissolved in dichloromethane (DCM) and washed with water; the organic layers were combined and dried over anhydrous Na_2SO_4. The solvent was removed under reduced pressure. The crude product was purified by column chromatography (silica gel, PE/DCM = 2:1, v/v) to give **1** as a light yellow solid (53.2 mg, yield: 25%). ^{1}H NMR (400 MHz, $CDCl_3$): δ = 9.95 (s, 1H), 7.80−7.73 (m, 5H), 7.51 (d, 1H, J = 4.0 Hz). EI-TOF-HRMS: calcd for $C_{12}H_7NOS^+$ m/z = 213.0248, found m/z = 213.0242.

2.3. Synthesis of TP-*meso*-BDP.[48] Thiophene-2-carbaldehyde (560.0 mg, 5.0 mmol) and 2,4-dimethylpyrrole (1 mL, 10.0 mmol) were dissolved in DCM (75 mL). After being purged with N_2 for 30 min, a few drops of trifluoroacetic acid were added to the solution and then the mixture was stirred at RT for 5 h. Then, dicyano-5,6-dichlorobenzoquinone (DDQ;

https://doi.org/10.1021/acs.jpcb.1c00053
J. Phys. Chem. B XXXX, XXX, XXX−XXX

1.0 g, 4.35 mmol) was added and the mixture was stirred. Dry triethylamine (TEA; 2 mL) was added after 0.5 h. The mixture was stirred for 15 min, $BF_3{\cdot}Et_2O$ (2 mL) was added dropwise under an ice bath. After stirring at RT overnight, the mixture was extracted with DCM and the organic layers were washed with water. The organic layers were combined, dried over anhydrous Na_2SO_4, and concentrated under reduced pressure. The crude product was purified by column chromatography (silica gel, PE/DCM = 2:1, v/v) to obtain compound **TP-*meso*-BDP** as an orange solid (165.0 mg, yield: 10%). ^{1}H NMR (400 MHz, $CDCl_3$): δ = 7.50 (dd, 1H, J_1 = 4.0 Hz, J_2 = 0.8 Hz), 7.14−7.12 (m, 1H), 6.99 (dd, 1H, J_1 = 4.0 Hz, J_2 = 0.8 Hz), 6.00 (s, 1H), 2.55 (s, 6H), 1.58 (s, 6H). EI-TOF-HRMS: calcd for $C_{17}H_{17}BF_2N_2S^+$ m/z = 330.1174, found m/z = 330.1182.

2.4. Synthesis of TP-CN-*meso*-BDP. **TP-CN-*meso*-BDP** was prepared by a method similar to that used for **TP-*meso*-BDP**. **TP-CN-*meso*-BDP** was obtained as an orange solid (38.9 mg, yield: 8%). Mp: >250 °C. ^{1}H NMR (400 MHz, $CDCl_3$): δ = 7.74−7.68 (m, 4H), 7.47 (d, 1H, J = 4.0 Hz), 7.03 (d, 1H, J = 4.0 Hz), 6.03 (s, 2H), 2.56 (s, 6H), 1.70 (s, 6H). ^{13}C NMR (100 MHz, $CDCl_3$): δ = 156.6, 144.1, 143.3, 137.7, 136.3, 132.9, 132.5, 132.2, 129.4, 126.1, 125.3, 121.8, 118.6, 111.3, 29.7, 14.7, 13.9. EI-TOF-HRMS: calcd for $C_{24}H_{20}BF_2N_3S^+$ m/z = 431.1439, found m/z = 431.1440.

2.5. Nanosecond Transient Absorption Spectroscopy. The nanosecond transient absorption spectra were measured on an LP980 laser flash photolysis spectrometer (Edinburgh Instruments, U.K.). The samples were excited with a nanosecond pulsed laser (Opolette; the wavelength is tunable in the range of 210−2400 nm; OPOTEK). The typical laser energy was ca. 5 mJ per pulse. The signal was digitized with a Tektronix TDS 3012B oscilloscope. All samples were deaerated with N_2 for ca. 15 min before measurement. The data (kinetic decay trace and spectrum) were processed with L900 software. The intrinsic triplet-state lifetime was obtained by fitting the experimental decay traces measured at different concentrations (preferably one with triplet−triplet annihilation (TTA), another with negligible TTA), using a kinetic model with the TTA effect considered.[54]

The triplet-state quantum yield was determined by the ground-state blenching (GSB) method, according to eq 1. In the equation, "sam" and "std" represent the sample and standard, respectively. Φ is the triplet-state quantum yield, ε is the molar absorption coefficient of the ground state determined by UV−vis absorption spectra, ΔA is the optical intensity of the ground-state bleaching band determined by nanosecond transient absorption spectra.

$$\Phi_{sam} = \Phi_{std}\left(\frac{\varepsilon_{std}}{\varepsilon_{sam}}\right)\left(\frac{\Delta A_{sam}}{\Delta A_{std}}\right) \quad (1)$$

2.6. Femtosecond Transient Absorption Spectroscopy. Femtosecond transient absorption spectra were measured on a system based on a Ti:sapphire regenerative amplifier (Amplitude Pulsar) producing 80 fs pulses centered at 810 nm with a repetition rate of 1 kHz and an average power of 450−500 mW. The regenerative amplifier was pumped by a homemade Ti:sapphire oscillator. The excitation pulses at 500 nm were produced by pumping an Optical Parametric Amplifier (TOPAS-Light Conversion) by a portion of the fundamental laser output. The white light continuum probe was obtained by focusing a small portion of the fundamental laser beam on a 3 mm thick CaF_2 window, which was kept rotating to avoid damage. All of the samples were contained in a quartz cell with a 2 mm optical path length. The samples were placed on a mobile stage to avoid photodegradation. The probe and the pump beam were set at magic angle polarization by rotating a $\lambda/2$ plate. Global fitting was performed with the GLOTARAN package using a linear sequential model.[55]

2.7. Fluorescence Quantum Yield (Φ_F). The fluorescence quantum yield was determined by **BDP-2** in toluene solution (Φ_F = 4.4%) as the standard following eq 2 (since most of the compounds give weak fluorescence, a standard also showing weak fluorescence was used to improve the determination accuracy). In the equation, sam and std represent the sample and standard, respectively. Φ is the fluorescence quantum yield, A is the absorbance of the excitation wavelength, F is the integral area of fluorescence, and η is the refractive index of used solvents.

$$\Phi_{sam} = \Phi_{std}\left(\frac{A_{std}}{A_{sam}}\right)\left(\frac{F_{sam}}{F_{std}}\right)\left(\frac{\eta_{sam}}{\eta_{std}}\right)^2 \quad (2)$$

2.8. Computation Details. Density functional theory (DFT) and time-dependent DFT (TDDFT) computations were carried out using the Gaussian 09 code.[56] The structures of all of the target compounds were fully optimized by the B3LYP[57,58] hybrid functional and the standard 6-31G(d) basis set. All of the structures were confirmed to be real minima by harmonic vibrational frequency calculations at the same level of theory. Triplet-state structures were obtained within the unrestricted DFT level. Solvent effects were considered by the nonequilibrium implementation of the polarizable continuum model in its linear response formalism[59,60] in a dichloromethane environment (ε = 8.93) since it evidenced the major differences between the chromophores. To provide an idea of the magnitude of the charge transferred within the chromophores, the index of the spatial extent method[61] is calculated using the Gaussian 16 code.[62] The value of transferred charges q_{CT} and the corresponding effective distance D_{CT} were thus used to confirm the existence of charge-separated state (CSS).

Further insights into the excited-state dynamics of all of the target compounds were obtained by performing geometry optimizations in vacuum at the TD CAM-B3LYP/6-31G(d) level of theory,[58] suggested as one of the best exchanges and correlation functionals for describing charge-transfer systems.[60,63] Semirelaxed potential energy surface (PES) scans for the rotation around the C−C thienyl linkers of the first excited state S_1 and the corresponding ground state were furthermore performed.

Spin−orbit matrix elements were calculated by the atomic-mean field approximation[64] as implemented in the DALTON code.[65] Since DALTON offers a limited choice of hybrid XC functionals, B3LYP was selected in conjunction with the cc-pVDZ basis set for all of the atoms. The spin−orbit couplings (SOCs) were defined according to the following formula

$$SOC_{nm} = \sqrt{\sum_i |\langle \psi S_n | \hat{H}_{SO} | \psi S_m \rangle|_i^2} \quad i = x, y, z \quad (3)$$

the $\hat{H}$ is the spin−orbit Hamiltonian.

2.9. Singlet Oxygen Quantum Yield (Φ_Δ). The singlet oxygen quantum yield was determined by eq 4. In the equation, sam and std represent the sample and standard,

https://doi.org/10.1021/acs.jpcb.1c00053
J. Phys. Chem. B XXXX, XXX, XXX−XXX

Scheme 2. Synthesis of the Compounds[a]

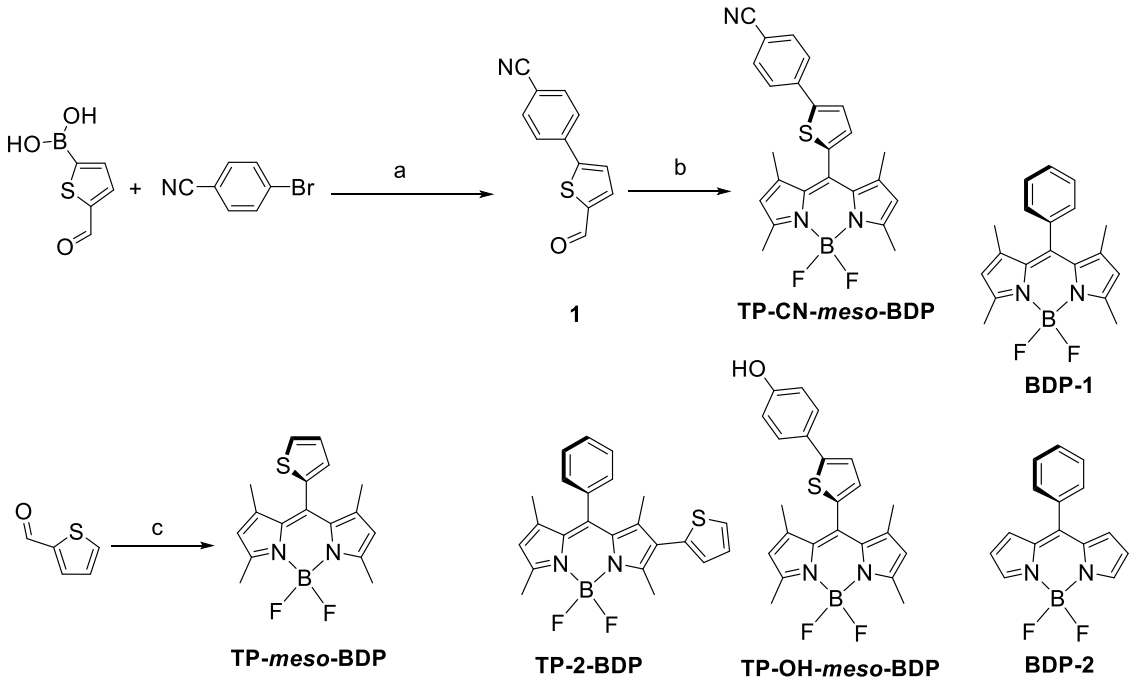

[a]Notes: (a) 5-formyl-2-thiopheneboronic acid, 4-bromocyanobenzene, $Pd(PPh_3)_4$, Na_2CO_3, dimethoxyethane (DME)/water, N_2, 4 h, yield: 25%. (b) 2,4-Dimethylpyrrole, trifluoroacetyl (TFA), RT for 5 h; DDQ, RT for 0.5 h; TEA, RT for 15 min; $BF_3{\cdot}Et_2O$, DCM, RT for overnight; N_2, yield: 8%. (c) 2,4-dimethylpyrrole, similar as step (b), yield: 10%. Compounds **1**, **BDP-1**, **BDP-2**, **TP-*meso*-BDP**, **TP-2-BDP** and **TP-OH-*meso*-BDP** are reported, **TP-CN-*meso*-BDP** is a new compound.

respectively. Φ is the singlet oxygen quantum yield, A is the absorbance at the excitation wavelength, k is the slope of the absorbance change of DPBF over time under photoexcitation, and η is the refractive index of used solvents.

$$\Phi_{sam} = \Phi_{std}\left(\frac{A_{std}}{A_{sam}}\right)\left(\frac{k_{sam}}{k_{std}}\right)\left(\frac{\eta_{sam}}{\eta_{std}}\right)^2 \quad (4)$$

3. RESULTS AND DISCUSSION

3.1. Molecular Structure Design and Synthesis. Thienyl moieties have been used as electron donors or electron-transfer bridges in organic materials used in photovoltaics and organic light-emitting diodes (OLEDs).[64,66,67] Bodipy derivatives with fused thiophene units have been reported, which show large spin−orbit coupling (SOC) matrix elements and efficient ISC.[68,69] Bodipy derivatives with a thiophene moiety attached were also reported, but for these compounds, no efficient ISC was found.[47,70,71] Herein, we synthesized two dyads with the thiophene moiety linked at two different positions on the Bodipy core, **TP-*meso*-BDP** and **TP-2-BDP** (Scheme 2).[47−49,72] The interesting points are that the fluorescence of **TP-*meso*-BDP** is quenched by torsion at S_1 state (which is different from the *meso*-phenyl Bodipy analogue), whereas this torsion is inhibited by fast charge separation and SOCT-ISC in **TP-2-BDP**. Furthermore, we linked either a 4′-hydroxylphenyl group (**TP-OH-*meso*-BDP**)[72] or a 4′-cyanophenyl moiety (strong electron-withdrawing group) to the thienyl unit to tune the electron-donating ability (**TP-CN-*meso*-BDP**). These two compounds were used as reference compounds (**TP-2-BDP** and **TP-CN-*meso*-BDP**) in the photophysical studies.

Thiophene was connected to the 4′-hydroxylphenyl group and 4′-cyanophenyl moiety by Suzuki−Miyaura crossing coupling reactions (Scheme 2). The typical Bodipy synthesis process was used to prepare the molecules **TP-*meso*-BDP**, **TP-OH-*meso*-BDP**, and **TP-CN-*meso*-BDP**.[37] **TP-2-BDP** was prepared by Suzuki−Miyaura crossing coupling reactions.[73] All molecular structures were confirmed by NMR and HRMS (Supporting Information). **TP-*meso*-BDP** was reported recently,[47−50] but the photophysical properties were not studied in detail.

3.2. UV−Vis Absorption Spectra. The UV−vis absorption spectra of the compounds are reported in Figure 1. The UV−vis absorption spectrum of **TP-*meso*-BDP** shows a slightly red-shifted band as compared with the reference **BDP-1**, indicating a small electronic interaction between the Bodipy and thienly moieties at the ground state. For **TP-2-BDP**, the absorption is red-shifted and broad, which can be

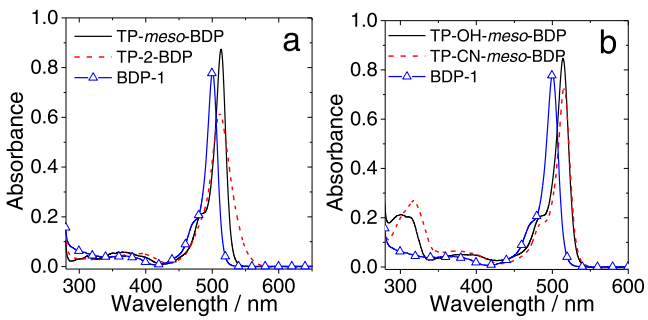

Figure 1. UV−vis absorption spectra of (a) **BDP-1**, **TP-*meso*-BDP**, and **TP-2-BDP** and (b) **BDP-1**, **TP-OH-*meso*-BDP**, and **TP-CN-*meso*-BDP**. c =1.0 × 10^{-5} M in DCM, 20 °C.

https://doi.org/10.1021/acs.jpcb.1c00053
J. Phys. Chem. B XXXX, XXX, XXX−XXX

attributed to an extended π-conjugation and an increased electron coupling between the Bodipy and its thienyl substituent. Indeed, based on DFT computations, we found that the dihedral angle between the *meso*-thienyl and the Bodipy unit is ca. 89.9° for **TP-*meso*-BDP**, whereas for **TP-OH-*meso*-BDP**, with the thienyl moiety at 2-position of Bodipy, the dihedral angle is 53.7° (vide infra). For **TP-OH-*meso*-BDP** , the absorption bands are narrow as compared to those for **TP-*meso*-BDP** and the reference compound **BDP-1** (Figure 1b), indicating that electronic interactions are very weak at the ground state.

3.3. Fluorescence Emission Spectra. The fluorescence emission spectra of the compounds were studied (Figure 2).

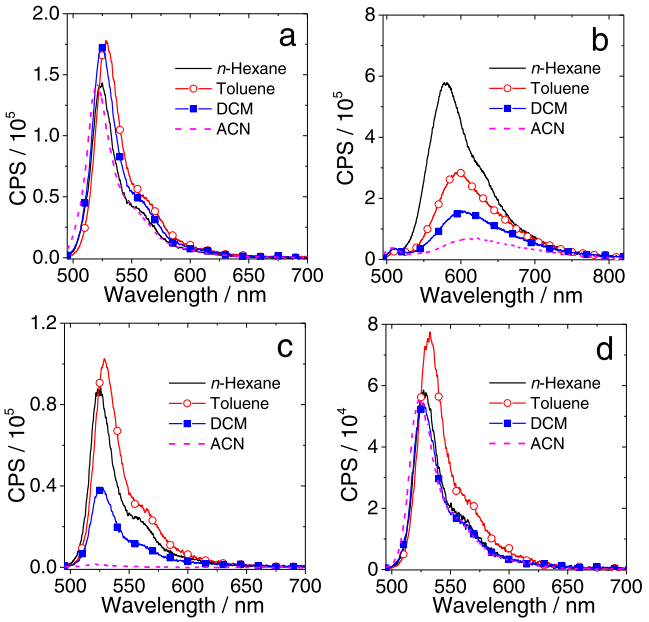

Figure 2. Fluorescence emission spectra of the compounds in different solvents. (a) **TP-*meso*-BDP**, (b) **TP-2-BDP**, (c) **TP-OH-*meso*-BDP**, and (d) **TP-CN-*meso*-BDP**. Optically matched solutions were used for comparison of the emission; λ_{ex} = 490 nm, A = 0.151, 20 °C.

For **TP-*meso*-BDP**, the emission band is centered at 524 nm (in DCM, Figure 2a) and the fluorescence quantum yield (Φ_F) is 6.7% in DCM, which is significantly lower than that for **BDP-1** (Φ_F = 72% in DCM). The quenching is independent of the solvent polarity (Table 1),[33] suggesting that it might be attributed to an intramolecular rotation (IMR) process rather than to charge separation.[49] The fluorescence is also quenched significantly compared to the simple Bodipy without substituent groups, **BDP-3** and **BDP-4** (Scheme S1), whose fluorescence quantum yields were reported as 92 and 89% in DCM, respectively.[74,75] For **TP-2-BDP**, a weak emission band at around 510 nm is observed in both polar and nonpolar solvents, which can be tentatively assigned as the localized excited state (LE) emission, and which is due to incomplete charge transfer. Meanwhile, a much stronger emission band is observed at longer wavelengths as compared with the LE emission. The intensity of this band and the overall fluorescence quantum yield decrease in polar solvents. For instance, the Φ_F was determined as 50.1% in *n*-hexane and decreased to 9.1% in acetonitrile (Table 1). The maximum of the long-wavelength band also shows a bathochromic shift as the solvent polarity is increased, which leads to its assignment as charge-separated state (CSS) emission (Figure 2b).

For **TP-OH-*meso*-BDP**, the emission is weak in nonpolar solvents such as *n*-hexane (Φ_F = 2.8%) and toluene (Φ_F = 3.9%) and it is further quenched in polar solvents, such as dichloromethane and acetonitrile (Φ_F = 1.9 and 0.01%, respectively) (Table 1 and Figure 2c). Solvent dependency of the fluorescence indicates that charge separation is an efficient process. The fluorescence is also quenched significantly for **TP-CN-*meso*-BDP** as compared with that for the reference **BDP-1** (Figure 2d and Table 1) (Φ_F = 71.2% for **BDP-1**).[16] For instance, the fluorescence quantum yield is only 3.7% in DCM. In this case, similar to what is observed for **TP-*meso*-BDP**, the fluorescence quantum yield is independent of solvent polarity, suggesting that also for this compound an IMR effect could be responsible for emission quenching.

The fluorescence decay kinetics in different solvents for all compounds were analyzed (Figure S16 and Table 1). For **TP-*meso*-BDP**, the fluorescence lifetime (0.39 ns in DCM) is shorter compared to that for **BDP-1** (3.7 ns) and it is independent of solvent polarity. The fluorescence lifetime of **TP-*meso*-BDP** is also much shorter as compared to those for the unsubstituted Bodipy compounds **BDP-3** and **BDP-4** (5.7 and 6.4 ns, respectively).[74,75] Similar results were observed for **TP-CN-*meso*-BDP**.

Different results were observed for **TP-2-BDP**. In this case, the LE emission lifetime is not sensitive to solvent polarity, but the CSS emission lifetime decreased along with increasing solvent polarity, from 4.7 ns in *n*-hexane to 1.6 ns in acetonitrile (Table 1). The reason is that the energy of the CSS becomes lower in polar solvents, and nonradiative transitions become more efficient (energy gap law). For **TP-OH-*meso*-BDP**, the emission lifetime was determined as 0.29 ns in toluene and decreased significantly in polar solvents (τ_F = 0.17 ns in acetonitrile), indicating that charge separation is efficient also for this compound.

Fluorescence quenching of **TP-*meso*-BDP** was previously associated with the greater rotation freedom of the thienyl group, as compared with the bulkier phenyl substituent.[47,49] It is known that the torsion of Bodipy substituents in the singlet excited state may enhance nonradiative decay.[41,42,46] To further prove this hypothesis, we studied the effect of viscosity on fluorescence emission (Figure 3). For **TP-*meso*-BDP**, the fluorescence quantum yield (Φ_F) increased from 5.5% in methanol (0.55 centipoise, cP) to 14.5% in glycol (17.3 cP) (Table S1). Meanwhile, the fluorescence lifetime increased from 0.73 to 1.3 ns (Table S1).

Similar results were obtained for **TP-CN-*meso*-BDP**: in this case, Φ_F is 17.6% in glycol ($E_T(30)$ = 56.3 kcal/mol), whereas Φ_F is 1.5% in methanol ($E_T(30)$ = 55.4 kcal/mol). In case charge separation is dominant for fluorescence quenching, the fluorescence intensity should be further quenched in the higher-polarity solvent glycol, while it is enhanced in the latter solvent, showing that the dominant effect is associated with solvent viscosity and not polarity.[76] The fluorescence intensity changed only slightly in highly viscous solvents for the reference compound **BDP-1** (Figure S18a). These results strongly indicate that the torsion of the thienyl substituent in the singlet excited state contributes to the fluorescence quenching of **TP-*meso*-BDP** and **TP-CN-*meso*-BDP**. As for the effect of viscosity, for **TP-2-BDP**, the LE emission is independent of solvent viscosity; however, the CT emission decreases in glycol, which is due to the polarity of this solvent

https://doi.org/10.1021/acs.jpcb.1c00053
J. Phys. Chem. B XXXX, XXX, XXX−XXX

Table 1. Photophysical Properties of Compounds

	solvent	λ_{abs}[a] (ε[b])	λ_F[c]	Φ_F[d]	τ_F[e]	Φ_Δ[f] (%)	Φ_T[g] (%)	τ_T[h]
TP-*meso*-BDP	HEX	513 (9.32)	524	5.3	0.74	[k]	[k]	128.0[l]
	TOL	516 (9.03)	528	6.2	0.70	[k]	[k]	270.4[l]
	DCM	513 (8.73)	524	6.7	0.39	[k]	[k]	210.5[l]
	ACN	509 (8.16)	520	4.8	0.65	[k]	[k]	96.6[l]
TP-2-BDP	HEX	510 (6.20)	508[i]/580[j]	0.6[i]/50.1[j]	3.0[i]/4.7[j]	7.4	6.2	130.1
	TOL	513 (6.12)	512[i]/595[j]	2.0[i]/32.3[j]	3.2[i]/3.3[j]	8.7	5.5	172.2
	DCM	511 (6.17)	509[i]/604[j]	2.1[i]/19.7[j]	3.4[i]/3.1[j]	7.3	7.2	139.1
	ACN	507 (4.89)	505[i]/613[j]	1.9[i]/9.1[j]	3.4[i]/1.6[j]	5.8	4.7	180.9
TP-OH-*meso*-BDP	HEX	514 (8.87)	524	2.8	0.27	0.7	1.9	228.9[m]
	TOL	517 (8.95)	529	3.9	0.29	4.6	8.1	700.4[m]
	DCM	514 (8.47)	524	1.9	0.24	44.1	45.3	247.3[m]
	ACN	510 (7.83)	524	0.01	0.17	17.5	15.6	338.3[m]
TP-CN-*meso*-BDP	HEX	516 (7.83)	527	2.3	0.24	[c]	1.8	236.5
	TOL	518 (7.44)	532	2.8	0.27	2.6	3.2	304.2
	DCM	515 (7.29)	526	3.1	0.29	1.2	4.6	482.5
	ACN	511 (6.95)	523	2.0	0.21	2.6	2.1	237.7

[a] $c = 1.0 \times 10^{-5}$ M, in nanometer. [b] Molar absorption coefficient. $\varepsilon = 10^4$ M^{-1} cm^{-1}. [c] In nanometer. [d] Fluorescence quantum yield, **BDP-2** in toluene (Φ_F = 4.4%) as the reference, λ_{ex} = 480 nm. [e] Fluorescence lifetime (λ_{ex} = 510 nm for **TP-*meso*-BDP**, **TP-OH-*meso*-BDP**, and **TP-CN-*meso*-BDP**; λ_{ex} = 445 nm for **TP-2-BDP**), in nanoseconds, $c = 1.0 \times 10^{-5}$ M. [f] Singlet oxygen quantum yield, 2,6-diiodoBodipy as the standard (Φ_Δ = 85% in toluene). [g] Triplet quantum yield, 2,6-diiodoBodipy as the standard (Φ_T = 88% in toluene). The discrepancy between the triplet-state quantum yields and the singlet oxygen quantum yields is due to experimental errors. [h] Triplet-state lifetime. [i] The transition of ^{1}LE → S_0. [j] The transition of ^{1}CSS → S_0. [k] Not observed. [l] Determined by the triplet−triplet energy transfer (TTET) method using PtOEP as a photosensitizer, in microseconds. [m] Intrinsic triplet-state lifetime, obtained by fitting experimental curves by the kinetic model with the TTA self-quenching effect considered,[54] in microseconds.

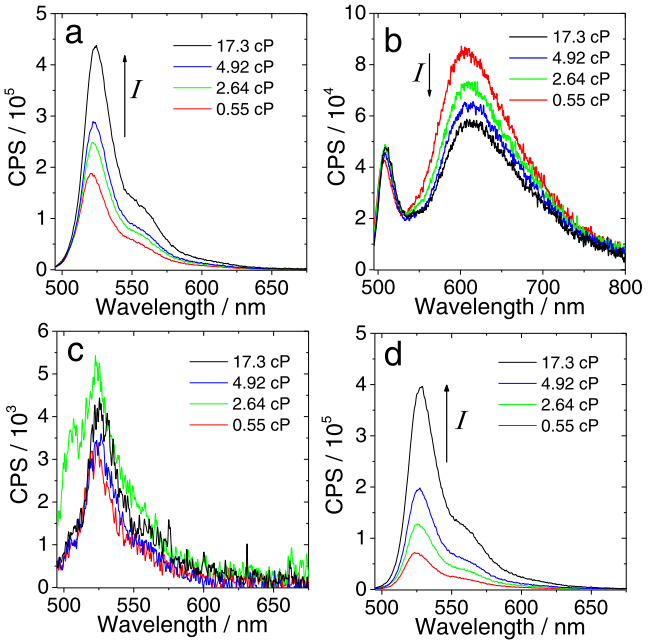

Figure 3. Change of fluorescence emission intensity in mixtures of methanol (E_T(30) = 55.4 kcal/mol) and glycol (E_T(30) = 56.3 kcal/mol) for (a) **TP-*meso*-BDP**, (b) **TP-2-BDP**, (c) **TP-OH-*meso*-BDP**, and (d) **TP-CN-*meso*-BDP** with increasing solvent viscosity. Optically matched solutions were used for comparison of the emission intensity; λ_{ex} = 490 nm, A = 0.179, 20 °C.

(Figure 3b). The fluorescence intensity and lifetime of **TP-OH-*meso*-BDP** show no obvious trend toward solvent viscosity (Figure 3c and Table S1).

We also analyzed the fluorescence behavior in nonpolar but highly viscous solvents. We used the low-polarity solvent poly(dimethylsiloxane) (PDMS; η = 489.9 cP) (E_T(30) = 32.5 kcal/mol), whose polarity is similar to that of toluene (E_T(30) = 33.9 kcal/mol; η = 0.59 cP). All of the four compounds showed intensified emission in PDMS, while the fluorescence intensity and lifetime of the reference compound **BDP-1** did not show any change (Figures S17 and S18b and Table S2). A longer fluorescence lifetime was observed for **TP-*meso*-BDP** and **TP-CN-*meso*-BDP** in PDMS, similar to what was observed in methanol/glycol, further supporting the idea of IMR quenching. For **TP-2-BDP** and **TP-OH-*meso*-BDP**, charge separation is thermodynamically allowed in toluene (vide infra). Since the polarity of PDMS is slightly lower than that of toluene, charge separation could be less efficient in this solvent.

As a preliminary evaluation of the ISC efficiency, we measured the singlet oxygen quantum yields of the compounds (Φ_Δ, Table 1). Φ_Δ values are generally low for all of the compounds, but interestingly, for **TP-OH-*meso*-BDP**, the Φ_Δ in DCM is as high as 44%. Since for this compound, charge separation is possible, we envision that charge recombination-induced ISC can be efficient.[77]

3.4. Electrochemical Characterization. To study the thermodynamics of charge separation, cyclic voltammetry was used to obtain the redox potentials (Figure 4). For **TP-*meso*-BDP**, an oxidation wave at +0.82 V and a reduction wave at −1.54 V were observed, respectively, which are attributed to the Bodipy moiety. For **TP-2-BDP**, we assume the irreversible oxidation wave at +0.44 V is due to the thiophene unit, and the reversible reduction wave at −1.64 V is due to the Bodipy moiety. For **TP-OH-*meso*-BDP**, an irreversible oxidation wave at +0.48 V was observed, as well as a reversible reduction wave at −1.57 V, indicating that the **TP-OH** moiety is the electron donor and the Bodipy is the electron acceptor. On the contrary, for **TP-CN-*meso*-BDP**, both the first oxidation wave at +0.79 V and the first reduction wave at −1.53 V can be attributed to the Bodipy, while the second oxidation wave at +1.37 V can be attributed to the **TP-CN** moiety.

https://doi.org/10.1021/acs.jpcb.1c00053
J. Phys. Chem. B XXXX, XXX, XXX−XXX

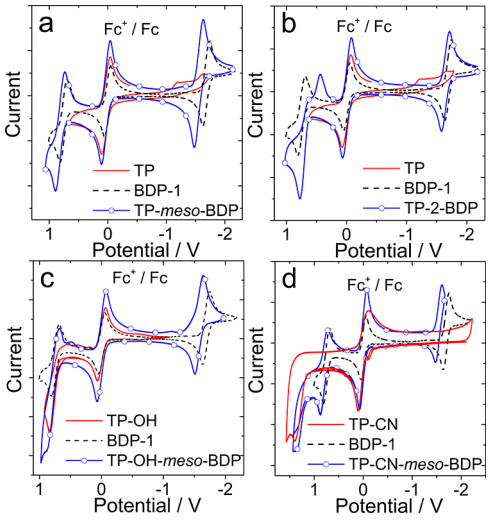

Figure 4. Cyclic voltammogram of the compounds: (a) **TP**, **BDP-1**, and **TP-*meso*-BDP**; (b) **TP**, **BDP-1**, and **TP-2-BDP**; (c) **TP-OH**, **BDP-1**, and **TP-OH-*meso*-BDP**; and (d) **TP-CN**, **BDP-1**, and **TP-CN-*meso*-BDP**. Ferrocene (Fc) was used as the internal reference. Condition: in deaerated DCM containing 0.10 M Bu_4NPF_6 as the supporting electrode, $Ag/AgNO_3$ as the reference electrode. Scan rates: 50 mV/s. $c = 1.0 \times 10^{-3}$ M, 20 °C.

The Weller equation was employed to calculate the Gibbs free energy changes for electron transfer and to estimate the energy of the charge-separated state (CSS) (Tables 2 and S3). Based on the Weller equation (eqs S1−S4), the Gibbs free energy changes for charge separation (ΔG_{CS}) can be obtained.

For **TP-*meso*-BDP**, using the reported oxidation potential of thiophene (+1.70 V), the calculated ΔG_{CS} values are all positive in nonpolar and polar solvents, indicating that charge separation is thermodynamically inhibited. The same conclusion is obtained for **TP-CN-*meso*-BDP** (Table 2). Opposite results are obtained for **TP-OH-*meso*-BDP**, for which the ΔG_{CS} values are negative in both nonpolar and polar solvents except in *n*-hexane, and for **TP-2-BDP**, indicating that charge separation is thermodynamically allowed. The calculated CSS energies are reported in Table 2.

3.5. Femtosecond Transient Absorption Spectroscopy. To unravel the excited state photophysics of all the studied compounds, femtosecond transient absorption (fs-TA) spectra were acquired (Figures 5 and 6). Previous studies of the reference compound **BDP-2** indicated a short-lived excited

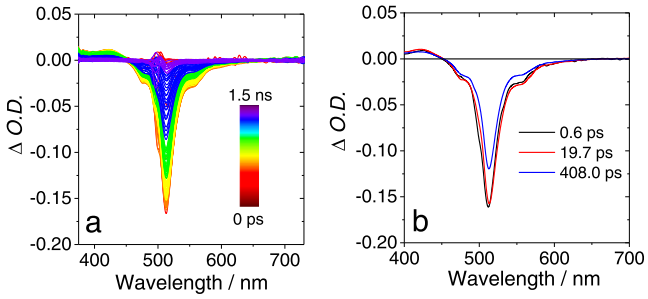

Figure 5. Femtosecond transient absorption spectra of **TP-*meso*-BDP**. (a) Transient absorption spectra at different delay times and (b) evolution-associated difference spectra (EADS). EADS were obtained by singular value decomposition (SVD) and global fitting. λ_{ex} = 500 nm, $c = 1.0 \times 10^{-5}$ M in DCM, 20 °C.

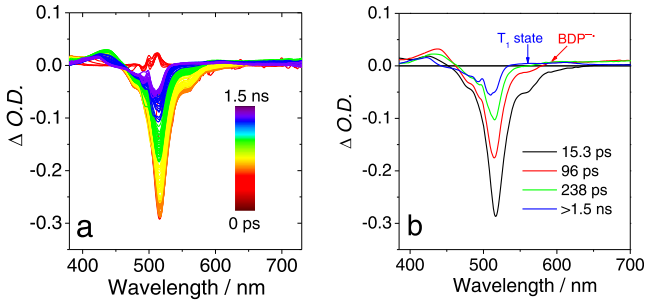

Figure 6. Femtosecond transient absorption spectra of **TP-OH-*meso*-BDP**. (a) Transient absorption spectra at different delay times and (b) evolution-associated difference spectra (EADS). EADS were obtained by singular value decomposition (SVD) and global fitting. λ_{ex} = 500 nm, $c = 1.0 \times 10^{-5}$ M in DCM, 20 °C.

state, whose rapid deactivation was assigned to solvent relaxation, vibrational relaxation, and geometry changes.[42,45,78]

For **TP-*meso*-BDP**, an intense negative band centered at about 515 nm was observed upon photoexcitation, which is assigned to the convolution of ground-state blenching (GSB) and stimulated emission (SE) bands (Figure 5a). A positive band centered at 430 nm was also observed, assigned to excited-state absorption (ESA). The ESA band shows a slight blue shift on the short timescale (ca. 1 ps), indicating solvent-induced relaxation of the Frank−Condon S_1 state. No Bodipy radical anion absorption band (should be at 585 nm) was observed in the fs-TA spectra, indicating that charge separation

Table 2. Electrochemical Redox Potentials, Driving Forces of Charge Separation (ΔG_{CS}), Charge Recombination (ΔG_{CR}), and the Energy of the Charge-Separated State (CSS) of the Compounds in Different Solvents[a]

			ΔG_{CS} (eV)				E_{CSS} (eV)			
	$E(ox)^b$/V	$E(red)^b$/V	HEX	TOL	DCM	ACN	HEX	TOL	DCM	ACN
TP-*meso*-BDP	+0.82	−1.54	+0.75	+0.66	+0.40	+0.33	3.19	3.10	2.84	2.77
TP-2-BDP	+0.44	−1.64	−0.01	−0.17	−0.64	−0.77	2.43	2.28	1.81	1.68
	+0.70									
TP-OH-*meso*-BDP	+0.48	−1.57	+0.04	−0.12	−0.58	−0.71	2.48	2.31	1.84	1.73
	+0.79									
TP-CN-*meso*-BDP	+0.79	−1.53	+0.73	+0.60	+0.25	+0.16	3.17	3.04	2.69	2.60
	+1.37									

[a]Cyclic voltammetry in N_2-saturated DCM containing a 0.10 M Bu_4NPF_6 supporting electrolyte; the counter electrode is the Pt electrode; the working electrode is the glassy carbon electrode; the $Ag/AgNO_3$ couple as the reference electrode. E_{00} is the energy approximated with the crossing point of UV−vis absorption and fluorescence emission after normalization at the singlet excited state, E_{00} = 2.44 eV. [b]The value is obtained by setting the oxidation wave of Fc^+/Fc as 0.

https://doi.org/10.1021/acs.jpcb.1c00053
J. Phys. Chem. B XXXX, XXX, XXX−XXX

unlikely contributes to the excited-state dynamics. The transient signal completely recovers within 1 ns due to the fast relaxation of the excited state. The results are different from what is observed for the reference compound **BDP-1**, showing an extended excited state lifetime (Figure S20a). The decay kinetics of **TP-*meso*-BDP** are instead similar to those measured for the reference compound **BDP-2** (Figure S20c).

To extract the time constants associated with the excited state evolution, a global fitting of the kinetic traces has been performed using a sequential linear decay scheme. The evolution-associated difference spectra (EADS) obtained from global analysis for **TP-*meso*-BDP** and **BDP-2** are reported in Figures 5b and S20d. For the reference compound **BDP-2**, two spectral components were obtained, with lifetimes of 15 and 291 ps, respectively. The process associated with the 15 ps component can be attributed to the solvent and vibrational relaxation, together with torsion of the phenyl moiety at the meso-position, in agreement with previous reports.[42,45] The 291 ps component is attributed to relaxation of the S_1 excited state, with a distorted, nonplanar geometry for the dipyrrin core, toward the ground state (Figure S20d).

In the case of **TP-*meso*-BDP**, global analysis retrieves three time constants with associated spectral components. The initial ultrafast 0.6 ps lifetime can be attributed to a fast solvent-induced relaxation process, bringing the system out of the initially reached Frank−Condon region. The following EADS, living for 19.7 ps can be associated with a geometry relaxation of the S_1 state, which might involve the rotation of the thiophene moiety and the distortion of the dipyrrin core. However, this relaxation is not reflected in any substantial variation of the band shape of the transient signal, which only shows a slight decrease in intensity during the evolution toward the last EADS. The lack of spectral evolution can be accounted for when considering that the structural relaxation involved in the excited state does not induce significant variation of the electronic distribution, as previously observed also in the case of **BDP-2**.[42] The lifetime of the final spectral component, 408 ps, is in good agreement with the fluorescence lifetime (0.39 ns, Table 1). Based on these results, we assume that the reason for the fluorescence quenching and short fluorescence lifetime of **TP-*meso*-BDP** is the same as that for **BDP-2**, i.e., rapid deactivation of the singlet excited state caused by the rotation of the thiophene moiety and distortion of the Bodipy core. Very similar deactivation kinetics of the singlet excited state were obtained for **TP-CN-*meso*-BDP** (Figure S23).

In the case of **TP-OH-*meso*-BDP**, charge separation is supposed to be responsible for the weak fluorescence, especially in polar solvents. The fs-TA spectra of **TP-OH-*meso*-BDP** indeed present several differences compared with **TP-*meso*-BDP** and **TP-CN-*meso*-BDP** (Figure 6). In this case, an intense negative band peaked at about 515 nm was also observed upon excitation, assigned to the convolution of GSB and SE, together with an ESA band peaked at about 420 nm. The initial spectral component extracted from global analysis (Figure 6b) can be attributed to the S_1 state reached upon excitation. Upon 15.3 ps (evolution from black to red EADS in Figure 6b), an intensity decrease of the negative band is observed, particularly on its red side. At the same time, the ESA band centered at 420 nm red-shifts to 440 nm, becoming more intense, and in the red part of the spectrum, a new band centered at 585 nm appears with low intensity. These spectral changes can be attributed to the formation of the radical anion of the Bodipy moiety, based on the previous literature.[79,80] In 96 ps, a decrease in intensity of the transient signal was observed (evolution from the red to the green trace in Figure 6b) assigned to structural relaxation of the molecule in the CSS. After 238 ps, the spectrum evolves toward the final spectral component (blue trace): here, a further decrease of the negative band and a variation of the ESA band initially peaked at 440 nm is observed, whose intensity substantially decays on its red side, determining the shift of its peak to 420 nm. The small positive band on the red part of the spectrum also changes in shape: its intensity vanishes at wavelengths longer than 630 nm, while it increases in the 520−670 nm spectral interval. These spectral changes indicate that a new species is formed on the 238 ps timescale: the comparison with the spectra acquired on a longer timescale (see infra, Figure 7a) allows the assignment of the final spectral component to the triplet state of **TP-OH-*meso*-BDP**. Therefore, based on the fit of the kinetic traces, we can determine the time constant ($k = 1/\tau$) of charge separation and charge recombination as 15.3 and 238 ps^{-1}, respectively. Since the species formed upon 238 ps is the triplet state of **TP-OH-*meso*-BDP**, we conclude that its formation occurs through the SOCT-ISC mechanism. These results agree with the large Φ_Δ values of **TP-OH-*meso*-BDP** in DCM (Table 1). The fs-TA spectra of **TP-OH-*meso*-BDP** were also measured in *n*-hexane (Figure S22). No absorption band of radical anions or radical cations was observed, confirming that charge separation is inhibited in this nonpolar solvent.

The fs-TA spectra of **TP-2-BDP** show that the charge separation occurs in DCM for this system (Figure S21). Two negative bands centered at 510 and 650 nm were observed, which can be assigned to the GSB and SE band, respectively. The radical anion signal of the Bodipy moiety located at around 570 nm was observed to rise within 1.2 ps. This band shows a small shift as compared with that reported for a Bodipy radical anion (585 nm) due to the overlap with the SE band. The time constant ($k = 1/\tau$) of charge separation was determined as 1.2 ps^{-1} based on the fit results (Figure S21b). The signals of the CSS state did not recover within the timescale of the measurement, indicating that the kinetic of charge recombination is slow.

3.6. Nanosecond Transient Absorption Spectroscopy: Triplet-State Properties. The triplet-state properties of the photosensitizers were analyzed by nanosecond transient absorption (ns-TA) spectroscopy (Figures 7 and S24−S26). As already mentioned, only **TP-OH-*meso*-BDP** showed a significant triplet quantum yield. For this compound, a ground-state blenching band (GSB) centered at 515 nm was observed upon pulsed laser excitation, together with two ESA bands, respectively, peaked at 420 nm and in the range from 520 to 650 nm: these spectral features are typical for the Bodipy triplet state.[81] The triplet-state quantum yield (Φ_T) was determined as 45% by the ground-state blenching method (refer to Section 2.5) and the apparent triplet-state lifetime (τ_T) as 104.3 μs in DCM. Due to the triplet−triplet annihilation (TTA) effect, the triplet-state lifetime will be shortened under the used experimental conditions. To determine the intrinsic triplet-state lifetime, the decay traces were fitted with a kinetic model with the TTA quenching effect considered and based on measurements of triplet lifetime at various concentrations.[54] With this method, the intrinsic triplet-state lifetime of **TP-OH-*meso*-BDP** was determined as 247.3 μs in DCM, which is shorter as compared with

https://doi.org/10.1021/acs.jpcb.1c00053
J. Phys. Chem. B XXXX, XXX, XXX−XXX

previously reported Bodipy triplet photosensitizers exploiting the SOCT-ISC mechanism.[82,83] For instance, the intrinsic triplet-state lifetimes of carbazole−Bodipy and phenoxazine−Bodipy are ca. 600 and 534 μs, respectively.[82,83] In other solvents, the Φ_T values of **TP-OH-*meso*-BDP** are lower than that in DCM, which is typical for photosensitizers based on the SOCT-ISC mechanism.

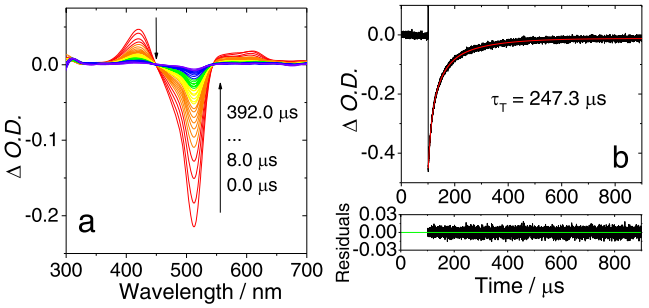

Figure 7. Nanosecond transient absorption spectra of **TP-OH-*meso*-BDP** in DCM. (a) transient absorption spectra and (b) decay trace at 515 nm. λ_{ex} = 510 nm, $c = 1.0 \times 10^{-5}$ M, 20 °C. The τ_T is the intrinsic lifetime obtained by fitting the data with a TTA-based kinetic model.

The sulfur atom of the thiophene may also contribute to the ISC of **TP-OH-*meso*-BDP**. To verify this possibility, we also measured the ns-TA spectra of **TP-*meso*-BDP**. No triplet-state signal was observed in all solvents for this compound (Table 1), except when iodoethane was added (Figure S27). These results demonstrate that the heavy atom effect of the thiophene moiety is negligible. Furthermore, if a phenol group is linked at 8-position (**BDP-OH**, Scheme S1), the ISC is also nonefficient (Table S4 and Figure S28) because charge separation is not occurring: this further supports the conclusion that the efficient ISC observed for **TP-OH-*meso*-BDP** in DCM is based on SOCT-ISC.

TP-CN-*meso*-BDP with the cyano group (electron withdrawing) was also studied (Table 1 and Figure S26). The highest Φ_T value is 4.6% in DCM (no obvious solvent polarity dependence was observed), which is much lower than the value observed for **TP-OH-*meso*-BDP** (Φ_T = 45% in DCM). All of the measurements for **TP-CN-*meso*-BDP** indicated that the electron-transfer process is inhibited because the electron-withdrawing −CN group weakens the electron-donating ability of the thiophene moiety, thus excluding the occurrence of SOCT-ISC. The triplet state of **TP-CN-*meso*-BDP** was observed to be long-lived (τ_T = 482.5 μs in DCM, Table 1) as well as that of **TP-*meso*-BDP** produced by the TTET method (τ_T = 210.5 μs in DCM, Table 1 and Figure S29).

3.7. DFT Computations. Further insights into the photophysics of the compounds came from the theoretical analysis. The ground-state geometries of the compounds were optimized with DFT computations (Figure 8). If the electron donor and acceptor adopt orthogonal orientations, the electron spin angular momentum changes will be compensated by the change of the molecular orbit angular momentum. Therefore, the orthogonal orientation between the electron donor and acceptor is normally favorable for enhancing the ISC in the case of SOCT-ISC.[32] For **TP-*meso*-BDP**, **TP-OH-*meso*-BDP**, and **TP-CN-*meso*-BDP**, the dihedral angles between Bodipy and thiophene moieties are almost 90° due to the steric hindrance of the methyl groups on the Bodipy. For **TP-2-BDP**, since the methyl groups at 1,3-position exert less steric hindrance toward the thiophene group as compared to that at 1,7-position, the conformation is more coplanar (dihedral angle 53.7°). The UV−vis absorption spectra of **TP-2-BDP** are red-shifted and broader than **BDP-1**, indicating an increased electronic coupling, which agrees with a more coplanar geometry and extended π-conjugation.

The frontier molecular orbitals of the compounds are presented in Figure 9. For **TP-*meso*-BDP** and **TP-CN-*meso*-BDP**, the lowest singlet excited state (S_1 state) corresponds to a HOMO → LUMO transition. The highest occupied molecular orbital (HOMO) and lowest unoccupied molecular orbital (LUMO) orbitals are both confined on the Bodipy moiety. For **TP-2-BDP**, the LUMO orbital is localized on the Bodipy moiety; however, delocalization from the Bodipy to the thienyl group is observed for the HOMO orbital due to the stronger electronic coupling between the two moieties. The effect of thienyl group on the LUMO energy is negligible, which is different from the thienyl-attached rhodamine dyes.[84] The large corresponding effective distance of charge transfer (D_{CT}) (2.20 Å) computed for the S_1 state confirms such a state as a CSS (Table S5).

For **TP-OH-*meso*-BDP**, the S_1 state is generated from the HOMO-1 → LUMO transition. The HOMO-1 and LUMO orbitals are localized on the Bodipy and **TP-OH** moieties, respectively, indicating that nonadiabatic charge separation is possible for **TP-OH-*meso*-BDP**, in agreement with the previously presented experimental findings (solvent polarity-dependent fluorescence and fs-TA spectra). The CSS character of the S_1 state is confirmed by the large D_{CT} value (5.491 Å) (Table S5). A large D_{CT} computed value is also observed in the T_2 state, while the T_1 state exhibits a very small value of D_{CT}. Therefore, the ISC should occur between S_1 (CSS) and T_1 (LE

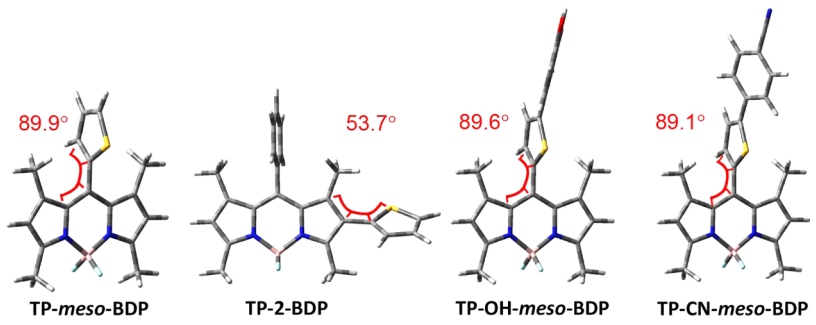

Figure 8. Optimized conformations and the dihedral angles of selected atoms of compounds calculated by DFT at the B3LYP/6-31G(d) level with Gaussian 09W based on the optimized ground state.

https://doi.org/10.1021/acs.jpcb.1c00053
J. Phys. Chem. B XXXX, XXX, XXX−XXX

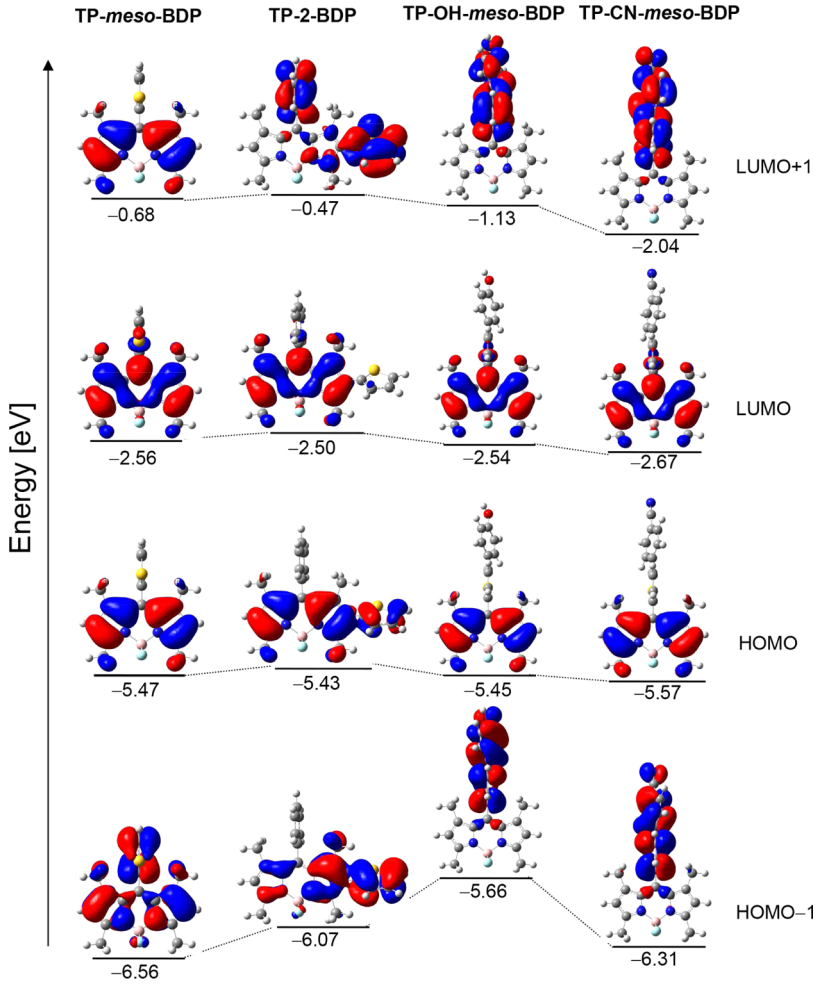

Figure 9. Selected frontier molecular orbitals and the energy (eV) of the dyads calculated by TDDFT at the B3LYP/6-31G(d) level with Gaussian 09W based on the optimized ground-state geometry. Isovalue = 0.02.

triplet state) states, as suggested also from the computed SOC values (Table S6).

The spin density surfaces of the triplet state were calculated (Figure S30). For **TP-2-BDP**, **TP-OH-*meso*-BDP**, and **TP-CN-*meso*-BDP**, the spin densities are localized on the Bodipy moiety, in agreement with the ns-TA spectra.

We also calculated the unrelaxed potential energy surface (PES) for the rotation of the C−C linker between the thienyl moiety and the Bodipy chromophore in the ground state (Figure 10). Different behaviors were observed: while for both **TP-OH-*meso*-BDP** and **TP-CN-*meso*-BDP**, the thermally accessible conformations are mainly in the region of 70−110°, which is beneficial to achieve an orthogonal orientation, and for **TP-2-BDP**, two minima were observed at around 60 and 120°, indicating that the preferential orientation is more planar (Figure 10a).

To attain more information about the anomalous fluorescence quenching of **TP-*meso*-BDP**, TDDFT calculations were used to perform the semirelaxed scan of the torsion angle of the S_1 state of **TP-*meso*-BDP** (Figure 11). By scanning the geometrical parameter accounting for thienyl orientation with respect to the Bodipy plane, the energy changes in the S_1 and ground states were monitored. As shown in Figure 11c, the semirelaxed ground-state potential energy surface scan evidences only one minimum structure, in which the *meso*-thienyl ring is almost orthogonal to the Bodipy core plane. The

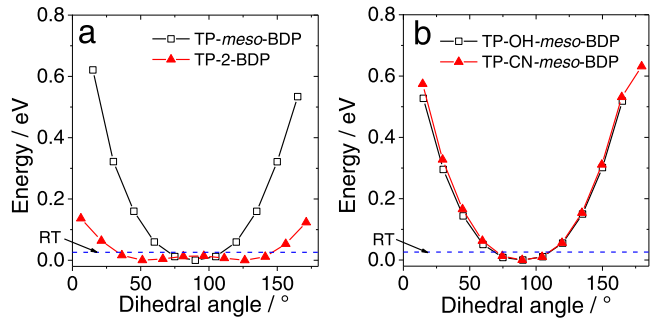

Figure 10. Unrelaxed potential energy surface scans of the ground states established by the rotation about the C−C linkers in (a) **TP-*meso*-BDP** and **TP-2-BDP** and (b) **TP-OH-*meso*-BDP** and **TP-CN-*meso*-BDP**.

PES of S_1 state (Figure 11c), instead, is smoother, indicating that a structural relaxation involving the thienyl rotation is easier.

It was previously found that in the case of a *meso*-vinyl-Bodipy, the fast nonradiative decay is due to the existence of a conical intersection (CI) between the S_1 and the S_0 potential energy surfaces and that a small energy barrier separates the Frank−Condon S_1 state and the minimum energy crossing point.[46] Furthermore, based on TDDFT/CASSCF computations, the distortion of the Bodipy core in the singlet excited

https://doi.org/10.1021/acs.jpcb.1c00053
J. Phys. Chem. B XXXX, XXX, XXX−XXX

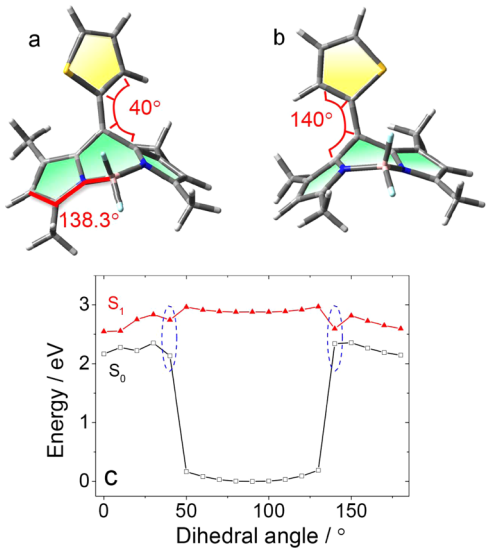

Figure 11. Optimized structures of the S_1 state with dihedral angles (between the thienyl moiety and the dipyrrin core) of (a) 40° and (b) 140° and (c) semirelaxed potential energy surface scans of the S_1 state and the corresponding ground-state energies established by the rotation around the C−C thienyl linkers in **TP-*meso*-BDP**. Conical intersections with GS are indicated by dashed blue ellipses. At these two conical intersections (CIs), the dipyrrin core takes a butterfly geometry, see (a) and (b).

state was proposed to be a butterfly-like motion, involving the bending over the boron-*meso*-C line.[46]

According to the PES of the S_1 state for **TP-*meso*-BDP**, changes of the dihedral angle from 130 to 140° and from 30 to 40° entail large structural changes in the core geometry (Figure 11c), leading the Bodipy core to assume a butterfly-like arrangement (Figure 11a,b). These structural changes are also accompanied by an abrupt decrease in oscillator strength for the electronic transition (e.g., from f = 0.4479, at 130°, to f = 0.0005, at 140°). Indeed, the bending of the boron atom with respect to the dipyrrin unit passes from 179.3°, in the GS minimum structure, to 138.3 and −161.6° in the S_1 structures obtained keeping fixed the scanned torsion angle to 40 and 140°, respectively (Figure 11a,b). Similar torsion was not observed for **BDP-1**, which is attributed to the bulky *meso*-phenyl substituent in **BDP-1**.

The proximity of the S_0 and S_1 state energies at the two molecular structures with the dihedral angles of 140 and 40° results in the formation of a CI for **TP-*meso*-BDP**. This suggests that a surface crossing can occur near these structural arrangements, similar to the other cases reported in the literature,[46] leading to fast inactivation of the S_1 state for **TP-*meso*-BDP** and weak fluorescence. Indeed, as determined by fs-TA spectroscopy, we propose the S_1 state decays in 408 ps, which is the timescale necessary to reach the CI (Figure 5).

Very similar behavior was found for **TP-CN-*meso*-BDP** (Figure S31), where the CI was found in correspondence of the same dihedral angles as for **TP-*meso*-BDP**. In conclusion, all our experimental and theoretical findings indicate that the IMR effect and the distortion of the Bodipy core in the excited determine the fluorescence quenching of **TP-*meso*-BDP** and **TP-CN-*meso*-BDP**, while efficient charge separation is the reason for quenching in the case of **TP-2-BDP** and **TP-OH-*meso*-BDP**.

3.8. Application of the Dyad in TTA Upconversion.

TTA upconversion (TTA-UC) is one of the important applications of triplet photosensitizers,[17] and recently, the heavy atom-free triplet photosensitizers have attracted much attention.[40] Due to the high ISC efficiency (Φ_T = 45% in DCM), long-lived triplet state (247.3 μs in DCM), and strong absorption of visible light ($\varepsilon = 8.5 \times 10^4$ M^{-1} cm^{-1} at 514 nm), **TP-OH-*meso*-BDP** was used as triplet PSs (energy donor) for TTA-UC with perylene used as an energy acceptor (annihilator, Figure 12). Without perylene, only the green

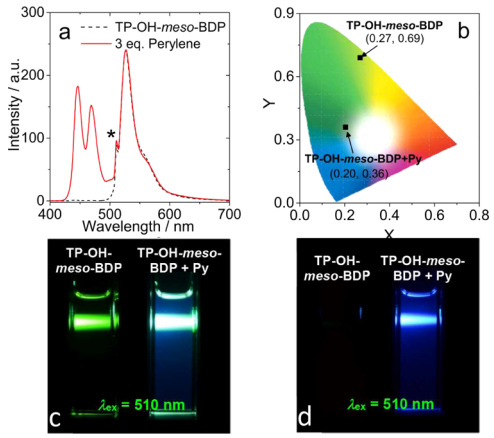

Figure 12. TTA upconversion with **TP-OH-*meso*-BDP** as the triplet photosensitizer and perylene (Py) as the acceptor, λ_{ex} = 510 nm (cw-laser). (a) Upconversion emission spectra. (b) Commission Internationale de l'Elcairage (CIE) diagram of the upconversion with **TP-OH-*meso*-BDP**. (c) Photographs of the emission of triplet photosensitizer alone and of upconversion. (d) Photographs of upconversion; the scattered laser and fluorescence are filtered by blue band pass filter (380−520 nm). Upconversion was performed upon excitation of the solution with a 510 nm continuous wave laser (power density, 53.2 mW/cm^2). The asterisks indicate the scattered laser. c (photosensitizer) = 1.0×10^{-5} M, c (acceptor) = 3.0×10^{-5} M, in DCM, 20 °C.

emission of **TP-OH-*meso*-BDP** (500−600 nm) was observed upon excitation with a 510 nm cw-laser. However, upconverted blue light (420−480 nm) of perylene was observed in the presence of 3.0 equiv of annihilator (Figure 12c). More significant color change was observed with a band pass filter (380−520 nm, Figure 12d). The upconversion quantum yield (Φ_{UC}) was determined as 6.0% in DCM.

The power-dependent upconversion spectra were also measured (Figure S33). From the logarithmic plot, a function of nearly slope 2 was obtained under low excitation power intensity, indicating a quadratic dependence between the intensities of excitation and upconverted emission. Upon increasing the excitation laser power, the relationship between the upconversion intensity and the excitation power density becomes linear. The threshold power density I_{th} reached 57.5 mW/cm^2.

Delayed fluorescence and triplet-state lifetime-based Stern−Volmer quenching were studied to characterize the TTA and TTET process using nanosecond transient absorption spectroscopy (Figure S32 and Table S7). In the presence of both **TP-OH-*meso*-BDP** and perylene, the TTA delayed fluorescence of perylene was observed (Figure S32). The rise kinetics (6.5 μs) can be mainly attributed to the TTET process, which leads to the generation and accumulation of the T_1 state of

https://doi.org/10.1021/acs.jpcb.1c00053
J. Phys. Chem. B XXXX, XXX, XXX−XXX

perylene, while the decreasing component (66.1 μs) originates from the TTA process (Figure S32b). Both are diffusion-controlled processes. The TTET process was analyzed with a Stern–Volmer quenching plot (Figure S32c), allowing us to obtain both the quenching constant (K_{SV}) (Table S7) and the TTET quantum yield and indicating that the TTET process is efficient.

The photophysical processes of **TP-OH-*meso*-BDP** are summarized in Scheme 3. Upon excitation of the Bodipy moiety, the S_1 state localized on this unit is initially populated. Subsequently, charge separation occurs (15.3 ps), leading to the population of a charge-separated state (CSS). Based on the weak coupling of the thienyl and Bodipy moieties, and the small overlap integral between the molecular orbitals of the two moieties, which is detrimental for radiative transition, the CSS should be a dark state (nonfluorescent). This conclusion explains the observed low fluorescence quantum yield of **TP-OH-*meso*-BDP**. Moreover, since the CSS energy is dependent on solvent polarity, also, the energy matching of the CSS state and the ^{3}LE state will change using solvents with different polarities. The distance between the electron donor and acceptor is short as compared to that of typical D-A systems used for radical pair ISC (RP-ISC; the ISC occurs from ^{1}CSS to ^{3}CSS). Thus, we expect the RP-ISC mechanism to be inhibited, and we conclude that ISC occurs between the ^{1}CSS and T_1 (LE triplet state) states. Since the T_2 state is a CSS, the ISC should occur between ^{1}CSS and T_1 (LE triplet state) states. In acetonitrile, the faster CR process will enhance the relaxation of the ^{1}CSS toward the ground state (Marcus-inverted region effect). Therefore, the triplet-state quantum yield in ACN (Φ_T = 15.6%) is lower than the value in DCM (Φ_T = 45.3%).

Scheme 3. Photophysical Processes of TP-OH-*meso*-BDP[a]

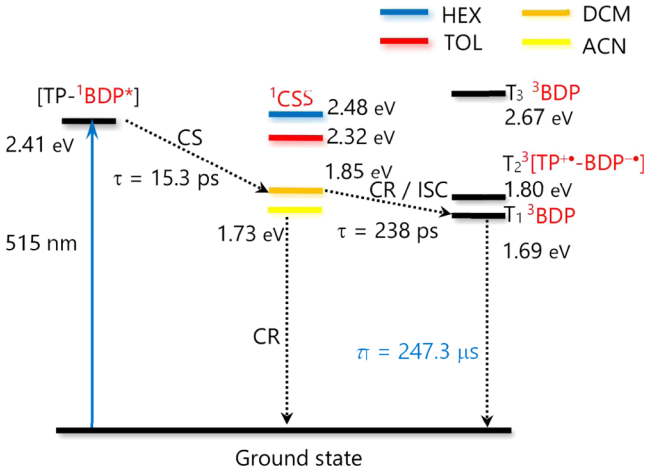

[a]The energy of the singlet state was determined by the UV–vis spectrum. The energy of CSS was determined by electrochemical calculations. The energy of the T_1 state of Bodipy was determined by the reported result.[85] The energy of the T_2 state was determined by the optimized T_2 geometry; the calculation was performed at the cam-B3LYP/6-31G(d) level with Gaussian 09W.

For **TP-*meso*-BDP**, the photophysical processes are different. Charge separation is unlikely due to the positive ΔG_{CS} values. Combining the observed fluorescence yield increase in viscous solvents (Figure 3a) and the results obtained by femtosecond transient absorption spectroscopy and DFT/TDDFT, we propose that the geometrical changes occurring at the S_1 state (19.7 ps) involving both a thienyl rotation and Bodipy core distortion and leading to a distorted geometry (lifetime, 408 ps; a dark state) are responsible for weak fluorescence (Table 1).

4. CONCLUSIONS

In summary, we prepared a series of thiophene–Bodipy dyads with electron donor or acceptor groups linked to the thienyl unit to study the excited-state dynamics and spin–orbit charge-transfer intersystem crossing (SOCT-ISC). The photophysical properties of the compounds were studied with steady-state and femtosecond/nanosecond transient absorption spectroscopy, as well as theoretical computations. For the compound with the thienyl moiety attached at the meso-position of Bodipy (**TP-*meso*-BDP**), anomalous weak fluorescence was observed in both nonpolar and polar solvents (quantum yield <6%). DFT computations indicate that the thienyl rotation and the Bodipy core distortion in the S_1 state open up a fast nonradiative drain decay channel, which is drastically different from what is observed for the *meso*-phenyl analogue. Femtosecond transient absorption spectral studies indicate that the geometrical changes occur within 19.7 ps and the distorted S_1 state decays within 408 ps. The same behavior was observed for **TP-CN-*meso*-BDP**, with an electron-withdrawing 4′-cyanophenyl group attached on the thienyl moiety. The behavior of **TP-OH-*meso*-BDP**, with an electron-donating 4′-hydroxylphenyl group on the thienyl unit, is completely different. In this case, the dyad shows fast charge separation (15.3 ps) and charge recombination and a high triplet yield in DCM, which supports the occurrence of a SOCT-ISC process (238 ps). In other words, the nonradiative decay channel of the *meso*-thienyl Bodipy is inhibited by the fast CS/CR-induced ISC, and the triplet-state quantum yield is up to 45% in DCM, with a triplet-state lifetime of up to 247.3 μs. The triplet-state quantum yield shows strong solvent polarity dependence (1.9–45%), as expected in the case of SOCT-ISC. Finally, the **TP-2-BDP** compound, where the thienyl group is linked at the 2-position, also undergoes efficient charge separation, but the ISC is not efficient. The dyad showing efficient SOCT-ISC (**TP-OH-*meso*-BDP**) was used as a heavy atom-free triplet photosensitizer for triplet–triplet annihilation upconversion. An upconversion quantum yield of up to 6% was observed. All of the results are useful for studying the excited-state dynamics of Bodipy chromophores, charge separation, and charge recombination in compact electron donor/acceptor dyads, as well as for the design of novel heavy atom-free triplet photosensitizers.

■ ASSOCIATED CONTENT

Supporting Information

The Supporting Information is available free of charge at https://pubs.acs.org/doi/10.1021/acs.jpcb.1c00053.

General experimental methods, molecular structure characterization, computational details, and additional spectra (PDF)

■ AUTHOR INFORMATION

Corresponding Authors

Jianzhang Zhao – *State Key Laboratory of Fine Chemicals, School of Chemical Engineering, Dalian University of*

https://doi.org/10.1021/acs.jpcb.1c00053
J. Phys. Chem. B XXXX, XXX, XXX–XXX

Technology, Dalian 116024, P. R. China; orcid.org/0000-0002-5405-6398; Email: zhaojzh@dlut.edu.cn

Gloria Mazzone − *Dipartimento di Chimica e Tecnologie Chimiche, Università della Calabria, I-87036 Arcavacata di Rende, Italy*; Email: gloria.mazzone@unical.it

Mariangela Di Donato − *LENS (European Laboratory for Non-Linear Spectroscopy), 50019 Sesto Fiorentino, Firenze, Italy; ICCOM-CNR, 50019 Sesto Fiorentino, Firenze, Italy;* orcid.org/0000-0002-6596-7031; Email: didonato@lens.unifi.it

Authors

Yu Dong − *State Key Laboratory of Fine Chemicals, School of Chemical Engineering, Dalian University of Technology, Dalian 116024, P. R. China;* orcid.org/0000-0001-6191-7857

Maria Taddei − *LENS (European Laboratory for Non-Linear Spectroscopy), 50019 Sesto Fiorentino, Firenze, Italy*

Sandra Doria − *LENS (European Laboratory for Non-Linear Spectroscopy), 50019 Sesto Fiorentino, Firenze, Italy; ICCOM-CNR, 50019 Sesto Fiorentino, Firenze, Italy;* orcid.org/0000-0002-9440-1643

Laura Bussotti − *LENS (European Laboratory for Non-Linear Spectroscopy), 50019 Sesto Fiorentino, Firenze, Italy*

Complete contact information is available at: https://pubs.acs.org/10.1021/acs.jpcb.1c00053

Notes

The authors declare no competing financial interest.

■ ACKNOWLEDGMENTS

J.Z. thanks the NSFC (U2001222, 21673031, 21761142005, and 21911530095) and the State Key Laboratory of Fine Chemicals (ZYTS201901) for financial support. G.M. thanks the Università della Calabria for financial support. M.D.D. thanks the support from the European Union's Horizon 2020 Research and Innovation Program under grant agreement no. 871124 Laserlab-Europe.

■ REFERENCES

(1) Celli, J. P.; Spring, B. Q.; Rizvi, I.; Evans, C. L.; Samkoe, K. S.; Verma, S.; Pogue, B. W.; Hasan, T. Imaging and Photodynamic Therapy: Mechanisms, Monitoring, and Optimization. *Chem. Rev.* **2010**, *110*, 2795−2838.

(2) Cakmak, Y.; Kolemen, S.; Duman, S.; Dede, Y.; Dolen, Y.; Kilic, B.; Kostereli, Z.; Yildirim, L. T.; Dogan, A. L.; Guc, D.; et al. Designing Excited States: Theory-Guided Access to Efficient Photosensitizers for Photodynamic Action. *Angew. Chem., Int. Ed.* **2011**, *50*, 11937−11941.

(3) Awuah, S. G.; You, Y. Boron Dipyrromethene (Bodipy)-Based Photosensitizers for Photodynamic Therapy. *RSC Adv.* **2012**, *2*, 11169−11183.

(4) Meijer, M. S.; Talens, V. S.; Hilbers, M. F.; Kieltyka, R. E.; Brouwer, A. M.; Natile, M. M.; Bonnet, S. NIR-Light-Driven Generation of Reactive Oxygen Species Using Ru(II)-Decorated Lipid-Encapsulated Upconverting Nanoparticles. *Langmuir* **2019**, *35*, 12079−12090.

(5) Deckers, J.; Cardeynaels, T.; Penxten, H.; Ethirajan, A.; Ameloot, M.; Kruk, M.; Champagne, B.; Maes, W. Near-Infrared BODIPY-Acridine Dyads Acting as Heavy-Atom-Free Dual-Functioning Photosensitizers. *Chem. - Eur. J.* **2020**, *26*, 15212−15225.

(6) Zhao, J.; Wu, W.; Sun, J.; Guo, S. Triplet Photosensitizers: From Molecular Design to Applications. *Chem. Soc. Rev.* **2013**, *42*, 5323−5351.

(7) DiSalle, B. F.; Bernhard, S. Orchestrated Photocatalytic Water Reduction Using Surface-Adsorbing Iridium Photosensitizers. *J. Am. Chem. Soc.* **2011**, *133*, 11819−11821.

(8) You, Y.; Nam, W. Photofunctional Triplet Excited States of Cyclometalated Ir(III) Complexes: Beyond Electroluminescence. *Chem. Soc. Rev.* **2012**, *41*, 7061−7084.

(9) Shi, L.; Xia, W. Photoredox Functionalization of C-H Bonds Adjacent to a Nitrogen Atom. *Chem. Soc. Rev.* **2012**, *41*, 7687−7697.

(10) Hari Prasad, D.; Burkhard, K. The Photocatalyzed Meerwein Arylation: Classic Reaction of Aryl Diazonium Salts in a New Light. *Angew. Chem., Int. Ed.* **2013**, *52*, 4734−4743.

(11) Le Vaillant, F.; Garreau, M.; Nicolai, S.; Gryn'ova, G.; Corminboeuf, C.; Waser, J. Fine-Tuned Organic Photoredox Catalysts for Fragmentation-Alkynylation Cascades of Cyclic Oxime Ethers. *Chem. Sci.* **2018**, *9*, 5883−5889.

(12) Reynal, A.; Forneli, A.; Martinez-Ferrero, E.; Sánchez-Díaz, A.; Vidal-Ferran, A.; O'Regan, B. C.; Palomares, E. Interfacial Charge Recombination between e^--TiO_2 and the I^-/I^{3-} Electrolyte in Ruthenium Heteroleptic Complexes: Dye Molecular Structure−Open Circuit Voltage Relationship. *J. Am. Chem. Soc.* **2008**, *130*, 13558−13567.

(13) Van Landeghem, M.; Lenaerts, R.; Kesters, J.; Maes, W.; Goovaerts, E. Impact of the Donor Polymer on Recombination via Triplet Excitons in a Fullerene-Free Organic Solar Cell. *Phys. Chem. Chem. Phys.* **2019**, *21*, 22999−23008.

(14) Getmanenko, Y. A.; Singh, S.; Sandhu, B.; Wang, C.-Y.; Timofeeva, T.; Kippelen, B.; Marder, S. R. Pyrrole[3,2-*d*:4,5-*d*′]Bisthiazole-Bridged Bis(Naphthalene Diimide)s as Electron-Transport Materials. *J. Mater. Chem. C* **2014**, *2*, 124−131.

(15) Schulze, T. F.; Schmidt, T. W. Photochemical Upconversion: Present Status and Prospects for Its Application to Solar Energy Conversion. *Energy Environ. Sci.* **2015**, *8*, 103−125.

(16) Zhao, J.; Xu, K.; Yang, W.; Wang, Z.; Zhong, F. The Triplet Excited State of Bodipy: Formation, Modulation and Application. *Chem. Soc. Rev.* **2015**, *44*, 8904−8939.

(17) Zhou, J.; Liu, Q.; Feng, W.; Sun, Y.; Li, F. Upconversion Luminescent Materials: Advances and Applications. *Chem. Rev.* **2015**, *115*, 395−465.

(18) Yanai, N.; Kimizuka, N. New Triplet Sensitization Routes for Photon Upconversion: Thermally Activated Delayed Fluorescence Molecules, Inorganic Nanocrystals, and Singlet-to-Triplet Absorption. *Acc. Chem. Res.* **2017**, *50*, 2487−2495.

(19) Flamigni, L.; Barbieri, A.; Sabatini, C.; Ventura, B.; Barigelletti, F. Photochemistry and Photophysics of Coordination Compounds: Iridium. In *Photochemistry and Photophysics of Coordination Compounds II*; Balzani, V.; Campagna, S., Eds.; Springer: Berlin, 2007; pp 143−203.

(20) Williams, J. A. G. Photochemistry and Photophysics of Coordination Compounds: Platinum. In *Photochemistry and Photophysics of Coordination Compounds II*; Balzani, V.; Campagna, S., Eds.; Springer: Berlin, 2007; pp 205−268.

(21) Turro, N. J.; Scaiano, J. C.; Ramamurthy, V. *Principles of Molecular Photochemistry: An Introduction*; University Science Books, 2009.

(22) Gorman, A.; Killoran, J.; O'Shea, C.; Kenna, T.; Gallagher, W. M.; O'Shea, D. F. In Vitro Demonstration of the Heavy-Atom Effect for Photodynamic Therapy. *J. Am. Chem. Soc.* **2004**, *126*, 10619−10631.

(23) Chen, H.-C.; Hung, C.-Y.; Wang, K.-H.; Chen, H.-L.; Fann, W. S.; Chien, F.-C.; Chen, P.; Chow, T. J.; Hsu, C.-P.; Sun, S.-S. White-Light Emission from an Upconverted Emission with an Organic Triplet Sensitizer. *Chem. Commun.* **2009**, *267*, 4064−4066.

(24) Kamkaew, A.; Lim, S. H.; Lee, H. B.; Kiew, L. V.; Chung, L. Y.; Burgess, K. Bodipy Dyes in Photodynamic Therapy. *Chem. Soc. Rev.* **2013**, *42*, 77−88.

(25) Verhoeven, J. W. On the Role of Spin Correlation in the Formation, Decay, and Detection of Long-Lived, Intramolecular Charge-Transfer States. *J. Photochem. Photobiol., C* **2006**, *7*, 40−60.

(26) Ohkubo, K.; Fukuzumi, S. Rational Design and Functions of Electron Donor−Acceptor Dyads with Much Longer Charge-Separated Lifetimes than Natural Photosynthetic Reaction Centers. *Bull. Chem. Soc. Jpn.* **2009**, *82*, 303−315.
(27) KC, C. B.; Lim, G. N.; Nesterov, V. N.; Karr, P. A.; D'Souza, F. Phenothiazine−Bodipy−Fullerene Triads as Photosynthetic Reaction Center Models: Substitution and Solvent Polarity Effects on Photoinduced Charge Separation and Recombination. *Chem. - Eur. J.* **2014**, *20*, 17100−17112.
(28) Gibbons, D. J.; Farawar, A.; Mazzella, P.; Leroy-Lhez, S.; Williams, R. M. Making Triplets from Photo-Generated Charges: Observations, Mechanisms and Theory. *Photochem. Photobiol. Sci.* **2020**, *19*, 136−158.
(29) Dance, Z. E. X.; Mi, Q.; McCamant, D. W.; Ahrens, M. J.; Ratner, M. A.; Wasielewski, M. R. Time-Resolved EPR Studies of Photogenerated Radical Ion Pairs Separated by *p*-Phenylene Oligomers and of Triplet States Resulting from Charge Recombination. *J. Phys. Chem. B* **2006**, *110*, 25163−25173.
(30) Okada, T.; Karaki, I.; Matsuzawa, E.; Mataga, N.; Sakata, Y.; Misumi, S. Ultrafast Intersystem Crossing in Some Intramolecular Heteroexcimers. *J. Phys. Chem. A* **1981**, *85*, 3957−3960.
(31) van Willigen, H.; Jones, G.; Farahat, M. S. Time-Resolved EPR Study of Photoexcited Triplet-State Formation in Electron-Donor-Substituted Acridinium Ions. *J. Phys. Chem. V* **1996**, *100*, 3312−3316.
(32) Dance, Z. E. X.; Mickley, S. M.; Wilson, T. M.; Ricks, A. B.; Scott, A. M.; Ratner, M. A.; Wasielewski, M. R. Intersystem Crossing Mediated by Photoinduced Intramolecular Charge Transfer: Julolidine−Anthracene Molecules with Perpendicular π Systems. *J. Phys. Chem. A* **2008**, *112*, 4194−4201.
(33) Epelde-Elezcano, N.; Palao, E.; Manzano, H.; Prieto-Castañeda, A.; Agarrabeitia, A. R.; Tabero, A.; Villanueva, A.; de la Moya, S.; López-Arbeloa, Í.; Martínez-Martínez, V.; et al. Rational Design of Advanced Photosensitizers Based on Orthogonal Bodipy Dimers to Finely Modulate Singlet Oxygen Generation. *Chem. - Eur. J.* **2017**, *23*, 4837−4848.
(34) Gould, I. R.; Boiani, J. A.; Gaillard, E. B.; Goodman, J. L.; Farid, S. Intersystem Crossing in Charge-Transfer Excited States. *J. Phys. Chem. A* **2003**, *107*, 3515−3524.
(35) Colvin, M. T.; Ricks, A. B.; Scott, A. M.; Co, D. T.; Wasielewski, M. R. Intersystem Crossing Involving Strongly Spin Exchange-Coupled Radical Ion Pairs in Donor−Bridge−Acceptor Molecules. *J. Phys. Chem. A* **2012**, *116*, 1923−1930.
(36) Filatov, M. A.; Karuthedath, S.; Polestshuk, P. M.; Savoie, H.; Flanagan, K. J.; Sy, C.; Sitte, E.; Telitchko, M.; Laquai, F.; Boyle, R. W.; et al. Generation of Triplet Excited States via Photoinduced Electron Transfer in *meso*-Anthra-Bodipy: Fluorogenic Response toward Singlet Oxygen in Solution and in Vitro. *J. Am. Chem. Soc.* **2017**, *139*, 6282−6285.
(37) Chen, K.; Yang, W.; Wang, Z.; Iagatti, A.; Bussotti, L.; Foggi, P.; Ji, W.; Zhao, J.; Di Donato, M. Triplet Excited State of Bodipy Accessed by Charge Recombination and Its Application in Triplet−Triplet Annihilation Upconversion. *J. Phys. Chem. A* **2017**, *121*, 7550−7564.
(38) Zhao, Y.; Li, X.; Wang, Z.; Yang, W.; Chen, K.; Zhao, J.; Gurzadyan, G. G. Precise Control of the Electronic Coupling Magnitude between the Electron Donor and Acceptor in Perylenebisimide Derivatives via Conformation Restriction and Its Effect on Photophysical Properties. *J. Phys. Chem. C* **2018**, *122*, 3756−3772.
(39) Zhao, Y.; Duan, R.; Zhao, J.; Li, C. Spin−Orbit Charge Transfer Intersystem Crossing in Perylenemonoimide−Phenothiazine Compact Electron Donor−Acceptor Dyads. *Chem. Commun.* **2018**, *54*, 12329−12332.
(40) Wang, Z.; Zhao, J.; Di Donato, M.; Mazzone, G. Increasing the Anti-Stokes Shift in TTA Upconversion with Photosensitizers Showing Red-Shifted Spin-Allowed Charge Transfer Absorption but a Non-Compromised Triplet State Energy Level. *Chem. Commun.* **2019**, *55*, 1510−1513.
(41) Kuimova, M. K.; Yahioglu, G.; Levitt, J. A.; Suhling, K. Molecular Rotor Measures Viscosity of Live Cells Via Fluorescence Lifetime Imaging. *J. Am. Chem. Soc.* **2008**, *130*, 6672−6673.
(42) Suhina, T.; Amirjalayer, S.; Woutersen, S.; Bonn, D.; Brouwer, A. M. Ultrafast Dynamics and Solvent-Dependent Deactivation Kinetics of Bodipy Molecular Rotors. *Phys. Chem. Chem. Phys.* **2017**, *19*, 19998−20007.
(43) Guliyev, R.; Coskun, A.; Akkaya, E. U. Design Strategies for Ratiometric Chemosensors: Modulation of Excitation Energy Transfer at the Energy Donor Site. *J. Am. Chem. Soc.* **2009**, *131*, 9007−9013.
(44) Frath, D.; Massue, J.; Ulrich, G.; Ziessel, R. Luminescent Materials: Locking π-Conjugated and Heterocyclic Ligands with Boron(III). *Angew. Chem., Int. Ed.* **2014**, *53*, 2290−2310.
(45) Kee, H. L.; et al. Structural Control of the Photodynamics of Boron−Dipyrrin Complexes. *J. Phys. Chem. B* **2005**, *109*, 20433−20443.
(46) Prlj, A.; Fabrizio, A.; Corminboeuf, C. Rationalizing Fluorescence Quenching in *meso*-Bodipy Dyes. *Phys. Chem. Chem. Phys.* **2016**, *18*, 32668−32672.
(47) Gibbs, J. H.; Robins, L. T.; Zhou, Z.; Bobadova-Parvanova, P.; Cottam, M.; McCandless, G. T.; Fronczek, F. R.; Vicente, M. G. H. Spectroscopic, Computational Modeling and Cytotoxicity of a Series of *meso*-Phenyl and *meso*-Thienyl-Bodipys. *Bioorg. Med. Chem.* **2013**, *21*, 5770−5781.
(48) Cunha Dias de Rezende, L.; Menezes Vaidergorn, M.; Biazzotto Moraes, J. C.; da Silva Emery, F. Synthesis, Photophysical Properties and Solvatochromism of *meso*-Substituted Tetramethyl Bodipy Dyes. *J. Fluoresc.* **2014**, *24*, 257−266.
(49) Wang, H.; Vicente, M. G. H.; Fronczek, F. R.; Smith, K. M. Synthesis and Transformations of 5-Chloro-2,2′-Dipyrrins and Their Boron Complexes, 8-Chloro-Bodipys. *Chem. - Eur. J.* **2014**, *20*, 5064−5074.
(50) Rezende, L. C. D.; Emery, F. S. Fluorescence Quenching of Two *meso*-Substituted Tetramethyl Bodipy Dyes by Fe(III) Cation. *J. Braz. Chem. Soc.* **2015**, *26*, 1048−1053.
(51) Yu, C.; Miao, W.; Wang, J.; Hao, E.; Jiao, L. PyrrolylBodipys: Syntheses, Properties, and Application as Environment-Sensitive Fluorescence Probes. *ACS Omega* **2017**, *2*, 3551−3561.
(52) Ruan, Z.; Miao, W.; Yuan, P.; Le, L.; Jiao, L.; Hao, E.; Yan, L. High Singlet Oxygen Yield Photosensitizer Based Polypeptide Nanoparticles for Low-Power Near-Infrared Light Imaging-Guided Photodynamic Therapy. *Bioconjugate Chem.* **2018**, *29*, 3441−3451.
(53) Batista, R. M. F.; Costa, S. P. G.; Belsley, M.; Raposo, M. M. M. Synthesis and Optical Properties of Novel, Thermally Stable Phenanthrolines Bearing an Arylthienyl-Imidazo Conjugation Pathway. *Dyes. Pigm.* **2009**, *80*, 329−336.
(54) Lou, Z.; Hou, Y.; Chen, K.; Zhao, J.; Ji, S.; Zhong, F.; Dede, Y.; Dick, B. Different Quenching Effect of Intramolecular Rotation on the Singlet and Triplet Excited States of Bodipy. *J. Phys. Chem. C* **2018**, *122*, 185−193.
(55) Snellenburg, J. J.; Laptenok, S.; Seger, R.; Mullen, K. M.; Van Stokkum, I. H. M. Glotaran: A Java-Based Graphical User Interface for the *R* Package TIMP. *J. Stat. Software* **2012**, *49*, 1−22.
(56) Frisch, M. J.; T, G. W.; Schlegel, H. B.; Scuseria, G. E.; Robb, M. A.; Cheeseman, J. R.; Scalmani, G.; Barone, V.; Mennucci, B.; Petersson, G. A. et al. *Gaussian 09*, revision D.01; Gaussian, Inc.: Wallingford, CT, 2009.
(57) Lee, C.; Yang, W.; Parr, R. G. Development of the Colle-Salvetti Correlation-Energy Formula into a Functional of the Electron Density. *Phys. Rev. B* **1988**, *37*, 785−789.
(58) Yanai, T.; Tew, D. P.; Handy, N. C. A New Hybrid Exchange−Correlation Functional Using the Coulomb-Attenuating Method (CAM-B3LYP). *Chem. Phys. Lett.* **2004**, *393*, 51−57.
(59) Cossi, M.; Barone, V. Solvent Effect on Vertical Electronic Transitions by the Polarizable Continuum Model. *J. Chem. Phys.* **2000**, *112*, 2427−2435.
(60) Tomasi, J.; Mennucci, B.; Cammi, R. Quantum Mechanical Continuum Solvation Models. *Chem. Rev.* **2005**, *105*, 2999−3094.

https://doi.org/10.1021/acs.jpcb.1c00053
J. Phys. Chem. B XXXX, XXX, XXX−XXX

(61) Le Bahers, T.; Adamo, C.; Ciofini, I. A Qualitative Index of Spatial Extent in Charge-Transfer Excitations. *J. Chem. Theory Comput.* **2011**, *7*, 2498−2506.
(62) Frisch, M. J.; Trucks, G. W.; Schlegel, H. B.; Scuseria, G. E.; Robb, M. A.; Cheeseman, J. R.; Scalmani, G.; Barone, V.; Petersson, G. A.; Nakatsuji, H. et al. *Gaussian 16*, revision C.01; Gaussian, Inc.: Wallingford, CT, 2016.
(63) Zhao, Y.; Truhlar, D. G. Density Functional for Spectroscopy: No Long-Range Self-Interaction Error, Good Performance for Rydberg and Charge-Transfer States, and Better Performance on Average Than B3LYP for Ground States. *J. Phys. Chem. A* **2006**, *110*, 13126−13130.
(64) Zhao, Z.; Deng, C.; Chen, S.; Lam, J.; Qin, W.; Lu, P.; Wang, Z.; Kwok, H.; Ma, Y.; Qiu, H.; et al. Full Emission Color Tuning in Luminogens Constructed from Tetraphenylethene, Benzo-2,1,3-Thiadiazole and Thiophene Building Blocks. *Chem. Commun.* **2011**, *47*, 8847−8849.
(65) Aidas, K.; Angeli, C.; Bak, K.; Bakken, V.; Bast, R.; Boman, L.; Christiansen, O.; Cimiraglia, R.; Coriani, S.; Dahle, P.; et al. *Wiley Interdiscip. Rev.: Comput. Mol. Sci.* **2014**, *4*, 269−284.
(66) Liu, W.; Tang, A.; Chen, J.; Wu, Y.; Zhan, C.; Yao, J. Photocurrent Enhancement of Bodipy-Based Solution-Processed Small-Molecule Solar Cells by Dimerization via the *meso* Position. *ACS Appl. Mater. Interfaces* **2014**, *6*, 22496−22505.
(67) Nicolini, T.; Famulari, A.; Gatti, T.; Martí-Rujas, J.; Villafiorita-Monteleone, F.; Canesi, E. V.; Meinardi, F.; Botta, C.; Parisini, E.; Meille, S. V.; et al. Structure−Photoluminescence Correlation for Two Crystalline Polymorphs of a Thiophene−Phenylene Co-Oligomer with Bulky Terminal Substituents. *J. Phys. Chem. Lett.* **2014**, *5*, 2171−2176.
(68) Awuah, S. G.; Polreis, J.; Biradar, V.; You, Y. Singlet Oxygen Generation by Novel NIR Bodipy Dyes. *Org. Lett.* **2011**, *13*, 3884−3887.
(69) Ji, S.; Ge, J.; Escudero, D.; Wang, Z.; Zhao, J.; Jacquemin, D. Molecular Structure−Intersystem Crossing Relationship of Heavy-Atom-Free Bodipy Triplet Photosensitizers. *J. Org. Chem.* **2015**, *80*, 5958−5963.
(70) Hedley, G. J.; Ruseckas, A.; Benniston, A. C.; Harriman, A.; Samuel, I. D. W. Ultrafast Electronic Energy Transfer Beyond the Weak Coupling Limit in a Proximal but Orthogonal Molecular Dyad. *J. Phys. Chem. A* **2015**, *119*, 12665−12671.
(71) Wiebeler, C.; Plasser, F.; Hedley, G. J.; Ruseckas, A.; Samuel, I. D. W.; Schumacher, S. Ultrafast Electronic Energy Transfer in an Orthogonal Molecular Dyad. *J. Phys. Chem. Lett.* **2017**, *8*, 1086−1092.
(72) Chen, Y.; Zhao, J.; Guo, H.; Xie, L. Geometry Relaxation-Induced Large Stokes Shift in Red-Emitting Borondipyrromethenes (Bodipy) and Applications in Fluorescent Thiol Probes. *J. Org. Chem.* **2012**, *77*, 2192−2206.
(73) Wang, Z.; Zhao, J. Bodipy−Anthracene Dyads as Triplet Photosensitizers: Effect of Chromophore Orientation on Triplet-State Formation Efficiency and Application in Triplet−Triplet Annihilation Upconversion. *Org. Lett.* **2017**, *19*, 4492−4495.
(74) Zhang, X.-F.; Zhang, Y.; Xu, B. Enhance the Fluorescence and Singlet Oxygen Generation Ability of Bodipy: Modification on the *meso*-Phenyl Unit with Electron Withdrawing Groups. *J. Photochem. Photobiol., A* **2017**, *349*, 197−206.
(75) Zhang, X.-F.; Feng, N. Photoinduced Electron Transfer-Based Halogen-Free Photosensitizers: Covalent *meso*-Aryl (Phenyl, Naphthyl, Anthryl, and Pyrenyl) as Electron Donors to Effectively Induce the Formation of the Excited Triplet State and Singlet Oxygen for Bodipy Compounds. *Chem. - Asian J.* **2017**, *12*, 2447−2456.
(76) Toliautas, S.; Dodonova, J.; Žvirblis, A.; Čiplys, I.; Polita, A.; Devižis, A.; Tumkevičius, S.; Šulskus, J.; Vyšniauskas, A. Enhancing the Viscosity-Sensitive Range of a Bodipy Molecular Rotor by Two Orders of Magnitude. *Chem. - Eur. J.* **2019**, *25*, 10342−10349.
(77) Liang, H.; Sun, S.; Zafar, M.; Yuan, Z.; Dong, Y.; Ji, S.; Huo, Y.; Li, M.-D.; Zhao, J. Tuning the SOCT-ISC of Bodipy Based Photosentizers by Introducing Different Electron Donating Groups and Its Application in Triplet-Triplet-Annihilation Upconversion. *Dyes Pigm.* **2020**, *173*, No. 108003.
(78) Li, F. R.; Yang, S. I.; Ciringh, Y. Z.; Seth, J.; Martin, C. H.; Singh, D. L.; Kim, D. H.; Birge, R. R.; Bocian, D. F.; Holten, D.; et al. Design, Synthesis, and Photodynamics of Light-Harvesting Arrays Comprised of a Porphyrin and One, Two, or Eight Boron-Dipyrrin Accessory Pigments. *J. Am. Chem. Soc.* **1998**, *120*, 10001−10017.
(79) Hattori, S.; Ohkubo, K.; Urano, Y.; Sunahara, H.; Nagano, T.; Wada, Y.; Tkachenko, N. V.; Lemmetyinen, H.; Fukuzumi, S. Charge Separation in a Nonfluorescent Donor−Acceptor Dyad Derived from Boron Dipyrromethene Dye, Leading to Photocurrent Generation. *J. Phys. Chem. B* **2005**, *109*, 15368−15375.
(80) Lifschitz, A. M.; Young, R. M.; Mendez-Arroyo, J.; Roznyatovskiy, V. V.; McGuirk, C. M.; Wasielewski, M. R.; Mirkin, C. A. Chemically Regulating Rh(I)-Bodipy Photoredox Switches. *Chem. Commun.* **2014**, *50*, 6850−6852.
(81) Wu, W.; Guo, H.; Wu, W.; Ji, S.; Zhao, J. Organic Triplet Sensitizer Library Derived from a Single Chromophore (Bodipy) with Long-Lived Triplet Excited State for Triplet-Triplet Annihilation Based Upconversion. *J. Org. Chem.* **2011**, *76*, 7056−7064.
(82) Hou, Y.; Kurganskii, I.; Elmali, A.; Zhang, H.; Gao, Y.; Lv, L.; Zhao, J.; Karatay, A.; Luo, L.; Fedin, M. Electronic Coupling and Spin−Orbit Charge Transfer Intersystem Crossing (SOCT-ISC) in Compact BDP−Carbazole Dyads with Different Mutual Orientations of the Electron Donor and Acceptor. *J. Chem. Phys.* **2020**, *152*, No. 114701.
(83) Dong, Y.; Sukhanov, A. A.; Zhao, J.; Elmali, A.; Li, X.; Dick, B.; Karatay, A.; Voronkova, V. K. Spin−Orbit Charge-Transfer Intersystem Crossing (SOCT-ISC) in Bodipy-Phenoxazine Dyads: Effect of Chromophore Orientation and Conformation Restriction on the Photophysical Properties. *J. Phys. Chem. C* **2019**, *123*, 22793−22811.
(84) Sabatini, R. P.; Mark, M. F.; Mark, D. J.; Kryman, M. W.; Hill, J. E.; Brennessel, W. W.; Detty, M. R.; Eisenberg, R.; McCamant, D. W. A Comparative Study of the Photophysics of Phenyl, Thienyl, and Chalcogen Substituted Rhodamine Dyes. *Photochem. Photobiol. Sci.* **2016**, *15*, 1417−1432.
(85) Rachford, A. A.; Ziessel, R.; Bura, T.; Retailleau, P.; Castellano, F. N. Boron Dipyrromethene (Bodipy) Phosphorescence Revealed in $[Ir(ppy)_2(bpy\text{-}C{\equiv}C\text{-}Bodipy)]^+$. *Inorg. Chem.* **2010**, *49*, 3730−3736.

https://doi.org/10.1021/acs.jpcb.1c00053
J. Phys. Chem. B XXXX, XXX, XXX−XXX